Article

Current Biology

Molecular conflicts disrupting centromere maintenance contribute to *Xenopus* hybrid inviability

Graphical abstract

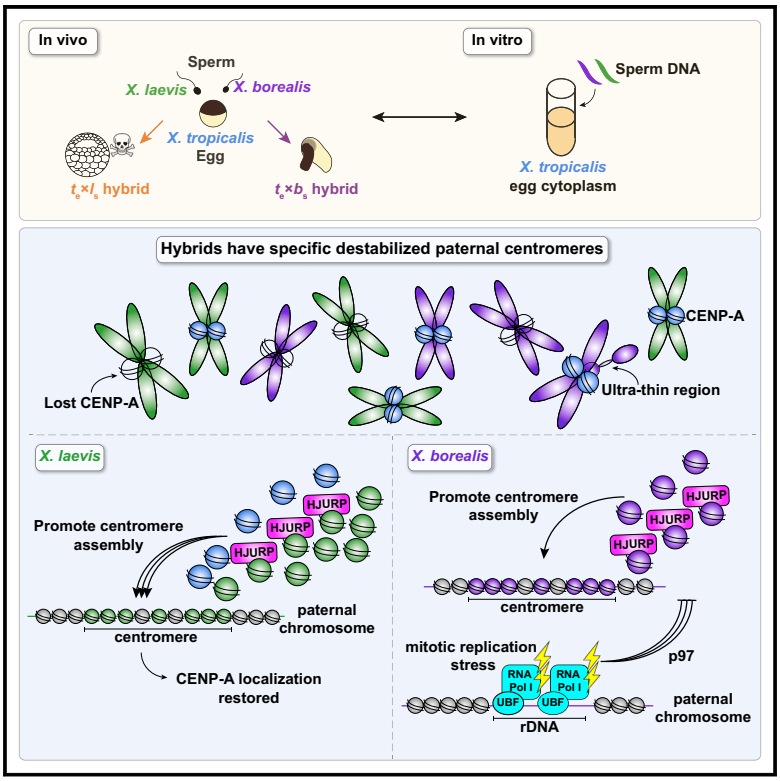

Highlights

- Divergent core centromeric sequences do not underlie *Xenopus* hybrid inviability
- CENP-A eviction from specific paternal chromosomes requires cell cycle progression
- Driving assembly can rescue and maintain *X. laevis*, but not *X. borealis*, centromeres
- Mitotic replication stress and conflicts lead to *X. borealis* chromosome defects

Authors

Maiko Kitaoka, Owen K. Smith, Aaron F. Straight, Rebecca Heald

Correspondence

bheald@berkeley.edu

In brief

Centromere incompatibilities in inviable *Xenopus* hybrids are DNA sequence independent and result from the disruption of epigenetic pathways required for CENP-A maintenance.

Kitaoka et al., 2022, Current Biology *32*, 3939–3951
September 26, 2022
https://doi.org/10.1016/j.cub.2022.07.037

CellPress

Current Biology

CellPress
OPEN ACCESS

Article

Molecular conflicts disrupting centromere maintenance contribute to *Xenopus* hybrid inviability

Maiko Kitaoka,[1] Owen K. Smith,[2] Aaron F. Straight,[2] and Rebecca Heald[1,3,4,*]
[1]Department of Molecular and Cell Biology, University of California, Berkeley, Berkeley, CA 94720-3200, USA
[2]Department of Biochemistry, Stanford University School of Medicine, Stanford, CA 94305-5307, USA
[3]Twitter: @rebeccaheald
[4]Lead contact
*Correspondence: bheald@berkeley.edu
https://doi.org/10.1016/j.cub.2022.07.037

SUMMARY

Although central to evolution, the causes of hybrid inviability that drive reproductive isolation are poorly understood. Embryonic lethality occurs when the eggs of the frog *X. tropicalis* are fertilized with either *X. laevis* or *X. borealis* sperm. We observed that distinct subsets of paternal chromosomes failed to assemble functional centromeres, causing their mis-segregation during embryonic cell divisions. Core centromere DNA sequence analysis revealed little conservation among the three species, indicating that epigenetic mechanisms that normally operate to maintain centromere integrity are disrupted on specific paternal chromosomes in hybrids. *In vitro* reactions combining *X. tropicalis* egg extract with either *X. laevis* or *X. borealis* sperm chromosomes revealed that paternally matched or overexpressed centromeric histone CENP-A and its chaperone HJURP could rescue centromere assembly on affected chromosomes in interphase nuclei. However, although the *X. laevis* chromosomes maintained centromeric CENP-A in metaphase, *X. borealis* chromosomes did not and also displayed ultra-thin regions containing ribosomal DNA. Both centromere assembly and morphology of *X. borealis* mitotic chromosomes could be rescued by inhibiting RNA polymerase I or preventing the collapse of stalled DNA replication forks. These results indicate that specific paternal centromeres are inactivated in hybrids due to the disruption of associated chromatin regions that interfere with CENP-A incorporation, at least in some cases due to conflicts between replication and transcription machineries. Thus, our findings highlight the dynamic nature of centromere maintenance and its susceptibility to disruption in vertebrate interspecies hybrids.

INTRODUCTION

Hybridization between closely related species often leads to embryonic lethality accompanied by defects in genome stability and maintenance, but the cellular and molecular mechanisms underlying post-zygotic barriers that drive reproductive isolation and speciation are largely unknown.[1–4] Among animals, a number of studies of inviable hybrids resulting from crosses of related *Drosophila* species have revealed an important role for the centromere, the chromosomal site where the kinetochore assembles to mediate chromosome attachment to the mitotic spindle and segregation to daughter cells. Both centromere DNA sequence and protein components including the centromeric histone H3 variant, centromere protein A (CENP-A) are rapidly evolving.[5,6] Localization of exogenously expressed CENP-A to centromeres across *Drosophila* species was shown to require co-expression of its species-matched chaperone CAL1/HJURP, indicating that the CENP-A deposition machinery co-evolves.[7] In turn, kinetochore formation at centromeres depends on specific, epigenetic recognition and stabilization of CENP-A nucleosomes by other factors, including CENP-C, CENP-N, and M18BP1.[8–16] Thus, co-evolution of centromere DNA and many associated proteins may generate barriers to hybrid viability by interfering with assembly of the chromosome segregation machinery.

Increasing evidence suggests that the chromatin environment also plays an important role in centromere assembly and that changes in nuclear organization are related to hybridization outcomes. For example, disruption of the chromocenter, a domain containing the pericentromeric satellite DNA, is common among *Drosophila* hybrids and may underlie inviability.[17] Furthermore, known inviability factors such as hybrid male rescue (Hmr) and lethal hybrid rescue (Lhr) strongly impact chromosome segregation in *Drosophila* hybrids and have been reported to regulate transposable elements and heterochromatic repeats,[18,19] associate with chromatin chaperones adjacent to centromeres,[20] and to link pericentromeric and centromeric chromatin to maintain centromere integrity.[21] However, whether these factors play a direct role in centromere function is unclear.[22] Despite these advances, the relative contribution to hybrid inviability of diverging centromere sequences versus the activity and spatial organization of

associated chromatin machineries that promote centromere assembly and maintenance is poorly understood.

Among vertebrates, hybridization resulting in post-zygotic death has been more difficult to study. *Xenopus* frog species possess interesting evolutionary relationships that include past interspecies hybridization events. For example, hybridization and whole-genome duplication of two *X. tropicalis*-like ancestors produced the allotetraploids *X. laevis* and *X. borealis*, which each contain two distinct subgenomes termed L (long) and S (short) to indicate overall differences in chromosome length.[23] These closely related *Xenopus* species provide an ideal system to study the molecular basis of hybridization outcomes, since cross fertilization experiments are easily performed,[24,25] and mechanisms underlying hybrid incompatibility can be uniquely and powerfully investigated *in vitro* by combining the sperm chromosomes and egg extracts from different species. We showed previously that interspecies hybrids produced when *X. laevis* or *X. borealis* eggs are fertilized by *X. tropicalis* sperm are viable, while the reverse crosses die before gastrulation and zygotic gene activation by explosive cell lysis or exogastrulation, respectively.[25] The inviable hybrids displayed chromosome segregation defects during embryonic cleavages, characterized by lagging chromosomes, chromosome bridges, and formation of micronuclei. By whole-genome sequencing, specific and distinct paternal chromosome regions were lost from both hybrids prior to embryo death. A fraction of *X. laevis* chromosomes failed to assemble centromeres/kinetochores, likely leading to spindle attachment defects and ultimately chromosome mis-segregation and embryo inviability.[25]

To better understand centromere-based *Xenopus* hybrid incompatibilities, here, we combine genomic, *in vitro*, and *in vivo* analyses. We find that although core centromeric sequences are not conserved, *X. tropicalis* egg cytoplasm supports centromere assembly on *X. laevis* and *X. borealis* chromosomes. However, upon entry into metaphase, conflicts emerge that evict CENP-A from a subset of chromosomes. In the case of *X. laevis*, excess CENP-A and its chaperone HJURP can rescue this defect. In contrast, eviction of CENP-A from *X. borealis* chromosomes could be rescued by dissociating rRNA Pol I or by preventing collapse of DNA replication forks. These results indicate that centromere incompatibility is driven primarily by centromere sequence-independent molecular conflicts that disrupt the epigenetic maintenance of CENP-A nucleosomes.

RESULTS

Core centromere sequence variation does not underlie *Xenopus* hybrid aneuploidy

We previously observed chromosome mis-segregation and loss of centromere and kinetochore proteins from a subset of chromosomes in hybrids generated by fertilizing *X. tropicalis* eggs with *X. laevis* sperm. Whole-genome sequencing just prior to embryo death revealed consistent deletion of large genomic regions from two paternal chromosomes, 3L and 4L of the L subgenome.[25] We hypothesized that chromosome-specific aneuploidy resulted from divergent centromeric sequences on the affected chromosomes, rendering them incompatible with the maternal *X. tropicalis* centromeric histone CENP-A and its loading machinery. Recent characterization of *X. laevis* centromere sequences by chromatin immunoprecipitation with CENP-A antibodies and sequencing analysis (ChIP-seq) revealed a family of related sequences found in distinct combinations and abundances on different *X. laevis* chromosomes.[26] However, *X. laevis* centromeres 3L and 4L did not possess any distinguishing features in terms of size or composition. Thus, differences in core centromere DNA sequences do not appear to drive the specific chromosome mis-segregation events and genome loss observed in the inviable *X. tropicalis*/*X. laevis* hybrid.

To expand our analysis, we characterized a second inviable hybrid resulting from fertilization of *X. tropicalis* eggs with sperm from *X. borealis*, a frog species possessing an allotetraploid genome closely related to *X. laevis*.[23] These hybrids display specific and consistent genome loss from a different subset of paternal chromosomes including 1S, 5S, 4L, and 8L.[25] To determine the extent to which centromere sequences differed across the three *Xenopus* species, CENP-A ChIP-seq was similarly applied to *X. tropicalis* and *X. borealis*. We used an alignment-independent *k*-mer based analysis to identify sequence features of the highly repetitive centromeric arrays in each species without the need for a complete genome sequence (Figure S1A). Comparing the enrichment value (normalized CENP-A *k*-mer counts/normalized input *k*-mer counts) revealed that the majority of individual *k*-mers are enriched in one species, but not the others (Figure 1A). Furthermore, analysis of full-length sequencing reads that contained CENP-A enriched *k*-mers showed that CENP-A nucleosome-associated DNA sequences of the three species bear little relationship to one another (Figure 1B). These findings reinforce the idea that incompatibilities leading to mis-segregation of specific chromosomes are not due to centromere sequence differences per se and are consistent with a vast literature showing that centromere function is defined epigenetically in most eukaryotes, including vertebrates.[27–29]

Interestingly, although protein sequence alignments of *X. laevis*, *X. tropicalis*, and *X. borealis* CENP-A showed that they are nearly 90% identical, divergence occurred in both the N terminus and the CENP-A-targeting domain (CATD) L1 loop region that provides specificity for recognition of the CENP-A/H4 complex by its dedicated chaperone HJURP[7,30–32] (Figure S1B). Together, these results suggest that as in *Drosophila*, CENP-A, and its chaperone may have co-evolved in *Xenopus* to strengthen the specificity of their interactions.[33] Importantly, however, although divergence and co-evolution of centromeres and associated proteins contributes to meiotic drive and can lead to hybrid inviability in flies,[34–36] such differences do not explain loss of centromere function on specific subsets of chromosomes in inviable *Xenopus* hybrids.

CENP-A eviction from a subset of chromosomes requires cell cycle progression

To better understand the process by which specific chromosomes lose centromere function in hybrids, we took advantage of the *Xenopus* egg extract system capable of recapitulating events of the embryonic cell division cycle *in vitro*. Interphase of these cell cycles lack gap (G) phases and consists entirely of S-phase when DNA replicates. During M-phase, chromosomes condense and assemble a kinetochore at

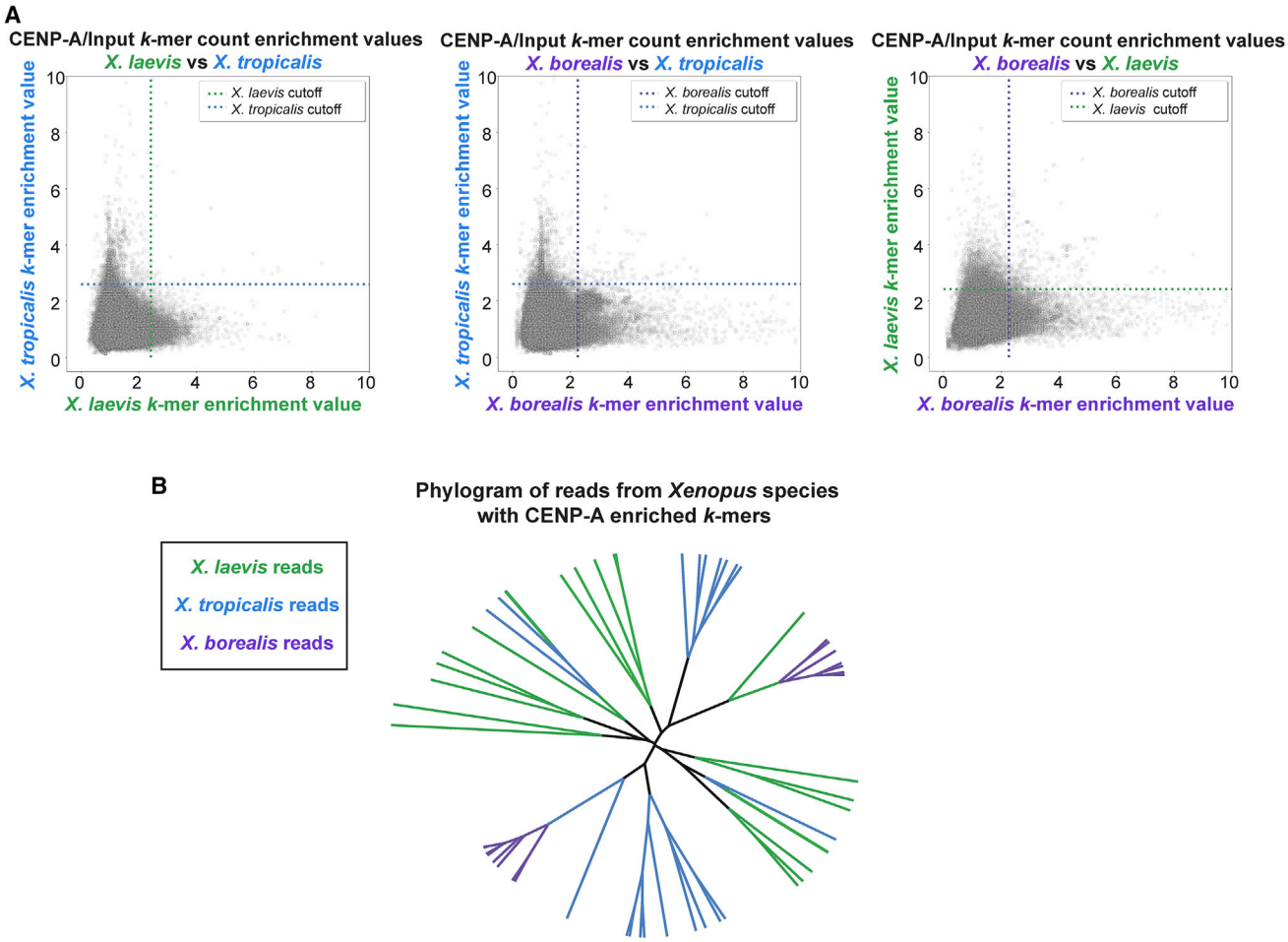

Figure 1. Comparison of *X. laevis*, *X. tropicalis*, and *X. borealis* core centromere sequences

(A) Scatter plots of *k*-mer enrichment values (normalized CENP-A counts/normalized input counts) compared between species. Only *k*-mers found in both species are plotted. Dotted lines indicate enrichment value for each species that is five median absolute deviations above the median enrichment value to denote highly enriched *k*-mers, which are not well conserved across species.

(B) Phylogram of full-length sequencing reads from each *Xenopus* species. Branches are colored according to species of origin. Sequencing reads were selected first by the presence of at least 80 CENP-A enriched 25 bp *k*-mers and then by hierarchical clustering. The phylogram illustrates a striking divergence of core centromere sequences.

See also Figure S1.

each centromere.[37,38] To monitor centromere assembly, *X. tropicalis*, *X. laevis*, or *X. borealis* sperm nuclei were added to *X. tropicalis* egg extracts and probed for CENP-A at different stages of the cell cycle. Sperm chromosomes of all three species condensed and possessed single centromeric CENP-A foci when added directly to metaphase-arrested *X. tropicalis* extract (Figures 2A and 2B), consistent with observations that sperm chromosomes contain CENP-A.[39,40] However, cycling the extract through interphase to allow sperm decondensation, nuclear envelope formation, and DNA replication in *X. tropicalis* egg cytoplasm resulted in no visible CENP-A on a subset of *X. laevis* and *X. borealis* mitotic chromosomes in the subsequent metaphase, whereas *X. tropicalis* centromeres were not affected (Figures 2A and 2B).

To determine when in the cell cycle CENP-A was evicted from paternal chromosomes, we examined interphase nuclei in control and hybrid *in vitro* reactions. The expected number of centromere foci, 18 for *X. laevis* and *X. borealis*, decreased in *X. tropicalis* extract (Figures 2C, S2A, and S2B). The loss of CENP-A localization from 2 or 4 paternal *X. laevis* and *X. borealis* chromosomes, respectively, corresponded very well to whole-genome sequencing data of hybrid embryos in terms of the number of chromosomes affected[25] and indicates that CENP-A is lost from this subset of paternal chromosomes during interphase.

The recent detailed characterization of *X. laevis* centromere sequences allowed us to test whether the centromere assembly defects observed in egg extract occurred on the same chromosomes disrupted in hybrid embryos.[25,26] Fluorescence *in situ* hybridization (FISH) probes in combination with CENP-A immunofluorescence identified *X. laevis* chromosomes 3L and 4L, the two chromosomes that lose large genomic regions in hybrid embryos, as those that also lose centromeric CENP-A staining when replicated in *X. tropicalis* egg extract (Figures S2C–S2E).

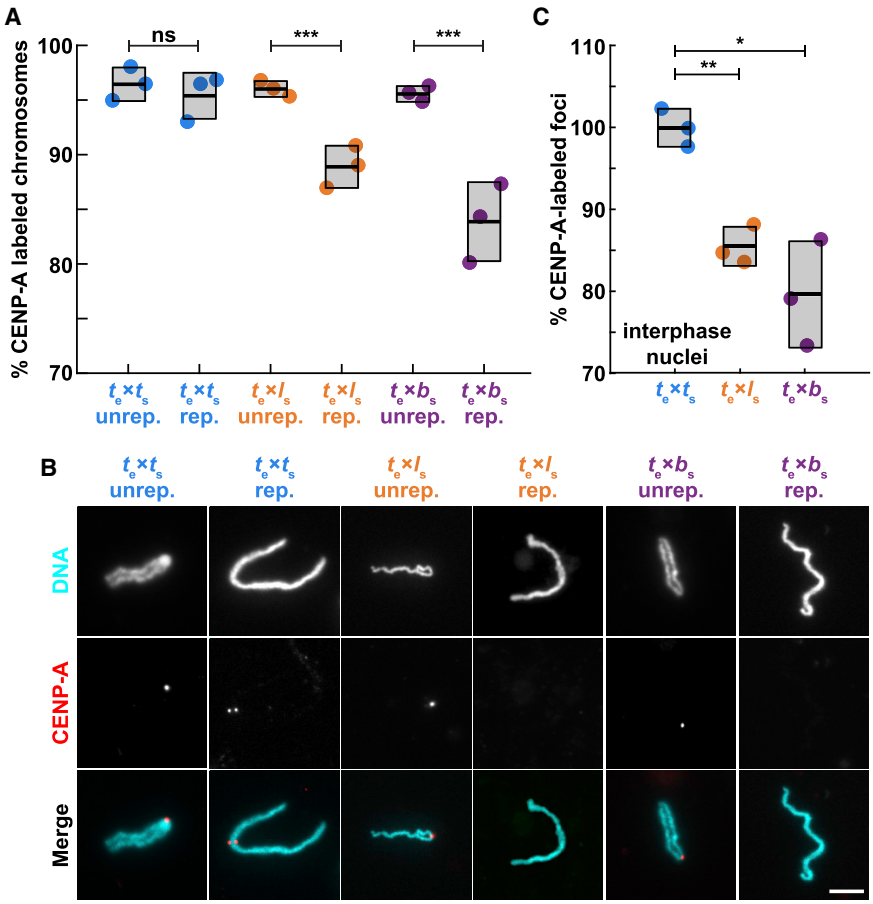

Figure 2. Loss of centromeric CENP-A is cell cycle dependent

(A) Percentage of mitotic chromosomes with centromeric CENP-A staining in *X. tropicalis* egg extract. Over 95% of *X. tropicalis*, *X. laevis*, and *X. borealis* unreplicated sperm chromosomes added directly to metaphase-arrested *X. tropicalis* egg extracts possess centromeres, as indicated by immunofluorescence of the centromeric histone CENP-A. Following progression through the cell cycle, a fraction of replicated *X. laevis* and *X. borealis* mitotic chromosomes completely lose centromeric CENP-A foci. Unrep, unreplicated chromosomes; rep, replicated chromosomes. n = 3 extracts, n > 275 chromosomes per extract. P values (left to right) by two-tailed two-sample unequal variance t tests: 0.3356, 0.0008, 0.0004; ns, not significant.

(B) Representative images of mitotic unreplicated and replicated *X. tropicalis*, *X. laevis*, and *X. borealis* chromosomes formed in *X. tropicalis* egg extracts. The chromosomes shown here are not identified but selected from a population of paternal chromosomes. DNA in cyan, CENP-A in red. Scale bar, 10 μm.

(C) Percentage of total expected CENP-A foci observed in nuclei formed in interphase *X. tropicalis* egg extract. *X. laevis* and *X. borealis* interphase nuclei both lose centromere foci during interphase, prior to entry into metaphase, whereas *X. tropicalis* nuclei do not. From n = 3 extracts, n > 64 nuclei per extract. P values (top to bottom) by one-way ANOVA with Tukey post hoc analysis: 0.0025 and 0.0133.

Species nomenclature throughout figures denotes egg extract as subscript e and chromosomes as subscript s; for example, t_e x l_s indicates *X. tropicalis* egg extract combined with *X. laevis* sperm chromosomes. *X. tropicalis* is color-coded blue, while *X. laevis* and *X. borealis* hybrid combinations are orange and purple, respectively.

See also Figure S2.

Thus, the *in vitro* system reproduces incompatibilities likely to underlie chromosome mis-segregation and ultimately genome loss observed *in vivo*. These results show that while all paternal sperm chromosomes initially possess CENP-A at their centromeres, a subset evict CENP-A during interphase, indicating that epigenetic mechanisms, likely involving the chaperone HJURP, operate to maintain CENP-A nucleosomes during DNA replication, as observed in cultured cells.[41] Such mechanisms enable hybrid centromere assembly despite evolutionary differences but are disrupted on specific individual chromosomes.

CENP-A and its chaperone HJURP can rescue *X. laevis* centromere assembly

We next sought to determine whether enhancing centromere assembly by adding species-matched paternal factors could prevent CENP-A eviction and centromere loss from specific *X. laevis* and *X. borealis* chromosomes formed in *X. tropicalis* extracts. *In vitro* reactions were supplemented with paternally matched proteins expressed in reticulocyte lysate, including CENP-A and its dedicated chaperone HJURP, at the onset of interphase (Figures S3A–S3C). Whereas adding *X. laevis* CENP-A resulted in a partial rescue, CENP-A plus HJURP increased the percentage of replicated *X. laevis* mitotic chromosomes with CENP-A foci to control levels (Figure 3A). In contrast, no combination of *X. borealis* centromere factors tested, including CENP-A, HJURP, and CENP-C,[42,43] restored CENP-A foci to replicated *X. borealis* mitotic chromosomes (Figure 3B). Notably, however, examination of interphase nuclei in *X. borealis* sperm/*X. tropicalis* egg extract reactions prior to metaphase entry revealed that CENP-A localization was initially fully rescued, with the expected number of CENP-A-positive foci corresponding to the number of chromosomes (Figure 3C). These results indicate that exogenous species-matched CENP-A and HJURP can restore proper centromere formation on all chromosomes during interphase of for both *X. laevis* and *X. borealis*, but that CENP-A is not maintained on a subset of *X. borealis* chromosomes upon entry into mitosis.

The ability to mix and match egg extract, sperm chromosomes, and exogenous centromere assembly factors enabled evaluation of CENP-A/centromere compatibilities across species. For example, despite striking differences in core centromere sequences between *X. laevis* and *X. borealis*

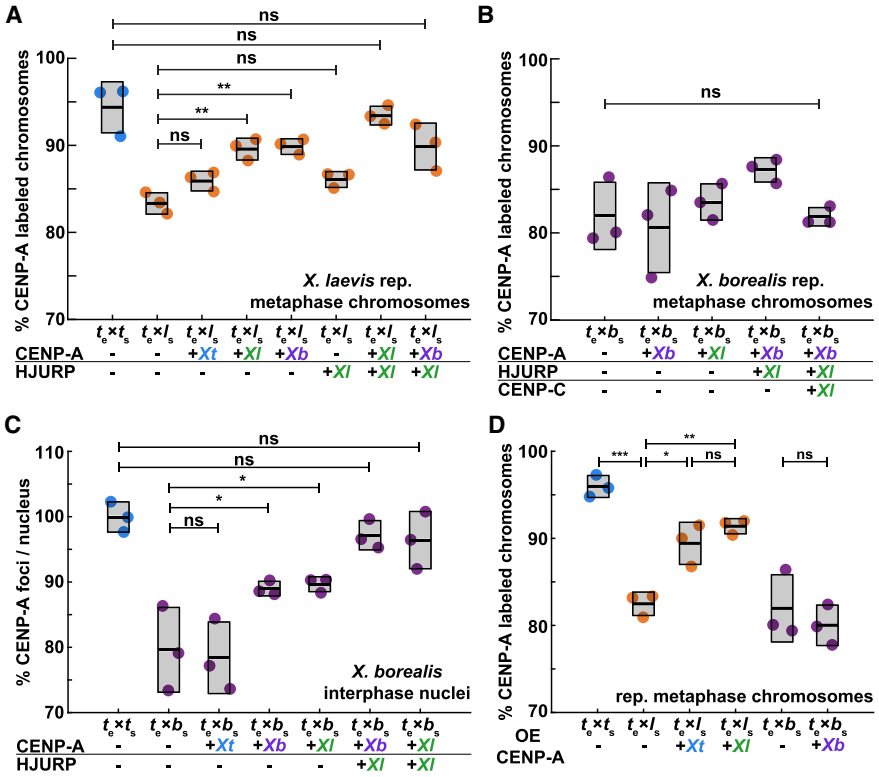

Figure 3. Driving CENP-A assembly rescues centromere localization in interphase, which persists on mitotic *X. laevis*, but not on *X. borealis*, chromosomes

(A) Percentage of replicated *X. laevis* chromosomes with centromeric CENP-A staining in *X. tropicalis* extract supplemented with *in-vitro*-translated CENP-A and HJURP proteins from different *Xenopus* species. *X. laevis* chromosomes are fully rescued with species-matched centromere proteins. Quantification with n = 3 extracts, n > 315 chromosomes per extract. p values (top to bottom) by one-way ANOVA with Tukey post hoc analysis: 0.1734, 0.9999, 0.5522, 0.0057, 0.0086, and 0.6281.

(B) Percentage of replicated *X. borealis* chromosomes with centromeric CENP-A staining in *X. tropicalis* extract supplemented with *in-vitro*-translated centromere proteins from different *Xenopus* species. No combination or increased amounts of centromeric proteins CENP-A (CA), HJURP (HJ), and CENP-C (CC) restored CENP-A localization on *X. borealis* mitotic chromosomes. Quantification with n = 3 extracts, n > 216 chromosomes per extract. p value by one-way ANOVA = 0.0786.

(C) Percentage of CENP-A-labeled centromeric foci in *X. borealis* nuclei assembled in *X. tropicalis* extract supplemented with *in-vitro*-translated centromere proteins from different *Xenopus* species. Driving centromere assembly with species-matched proteins fully restores formation of centromere foci in interphase, but CENP-A staining is subsequently lost in metaphase (B). Quantification with n = 3 extracts, n > 67 nuclei per extract. p values (top to bottom) by one-way ANOVA: 0.9996, 0.0562, 0.0433, 0.9690, and 0.9109.

(D) Percentage of replicated *X. laevis* or *X. borealis* chromosomes with centromeric CENP-A staining in *X. tropicalis* extract supplemented with excess (~80× endogenous levels) of *in-vitro*-translated *X. laevis* or *X. tropicalis* CENP-A. Whereas centromere staining is fully rescued on *X. laevis* mitotic chromosomes by CENP-A from either species, *X. borealis* centromere staining is not affected. Quantification with n = 3 extracts, n > 204 chromosomes per extract. p values (top to bottom, then left to right) by one-way ANOVA with Tukey post hoc analysis: 0.0042, 0.0001, 0.0249, 0.8845, and 0.88946.

(A–C) Centromere proteins were added at ~8× endogenous levels.

(A–D) ns, not significant.

See also Figure S3.

(Figure 1), the CATDs of the two species' CENP-A sequences are identical (Figure S1B), and exogenous CENP-A from either species equivalently restored centromere assembly on *X. laevis* mitotic chromosomes replicated in *X. tropicalis* egg extract (Figure 3A). Further, we observed that addition of excess exogenous *X. tropicalis* CENP-A could also increase the percentage of *X. laevis* mitotic chromosomes with centromere foci to control levels, although *X. borealis* chromosomes could not be rescued under any condition tested (Figures 3B and 3D). Together, our results indicate that enhancing the pathway that drives CENP-A incorporation into centromeric chromatin can fully overcome whatever is destabilizing centromeres on specific *X. laevis* centromeres and raised the question of why the *X. borealis* chromosomes are refractory to this rescue.

X. borealis chromosome defects result from mitotic replication stress

A clue as to why *X. borealis* mitotic chromosomes behave differently than *X. laevis* chromosomes in the *in vitro* hybrid extract system emerged with observation of their morphology. Although a subset of replicated *X. laevis* mitotic chromosomes formed in *X. tropicalis* extract lacked centromeres, they otherwise appeared normal. In contrast, 7%–10% of *X. borealis* mitotic chromosomes displayed ultra-thin regions of 2–3 μm

in length following replication, although centromeres on these chromosomes appeared largely intact (Figures 4A, 4B, S4A, and S4B). We reasoned that incomplete DNA replication leading to fork stalling and subsequent collapse in mitosis, termed replication stress, caused the formation of fragile sites.[44,45] Consistent with this idea, adding low doses of the DNA polymerase inhibitor aphidicolin that leads to replication stress[45–47] triggered formation of ultra-thin regions on *X. tropicalis* and *X. laevis* mitotic sperm chromosomes that had progressed through the cell cycle in *X. tropicalis* extract and slightly exacerbated morphological defects of *X. borealis* chromosomes (Figures S4C–S4E). Notably, however, the aphidicolin-induced replication stress did not affect CENP-A localization efficiency (Figure S4F), indicating that replication stress per se does not interfere with CENP-A loading and maintenance. Thus, under all conditions tested, we found no correlation between replication stress indicated by ultra-thin regions and defects in centromere assembly on the same chromosome (Figures S4B, S4E, and S4F).

To determine whether the *X. borealis* chromosome morphology and mitotic centromere defects were nevertheless linked, we treated the *in vitro* hybrid reactions with an inhibitor of the AAA ATPase p97 (Figure S4C). p97 is a multifunctional chaperone that removes the DNA replication helicase and causes collapse of stalled replication forks in mitosis.[45,48] Remarkably, we observed a complete rescue of both CENP-A localization and chromosome morphology on *X. borealis* chromosomes upon treatment with the p97 inhibitor (Figures 4C and 4D). Consistent with factors known to regulate the pathway of mitotic replication fork collapse and breakage,[45] Aurora A and Plk1 kinase inhibitors added to *X. tropicalis* extracts at low doses that avoided mitotic defects also rescued *X. borealis* chromosome morphology and CENP-A localization, but did not affect *X. laevis* or *X. tropicalis* chromosomes (Figures 4E and 4F). Finally, *X. laevis* or *X. tropicalis* chromosomes treated with aphidicolin followed by p97 inhibition displayed very few chromosome defects (Figures S4C and S4D). Combined, these data reveal that a subset of *X. borealis* chromosomes experience mitotic replication stress in *X. tropicalis* cytoplasm and that this is coupled to CENP-A eviction. However, centromere loss occurs on a different subset of mitotic chromosomes than those with ultra-thin regions.

Replication-transcription conflicts lead to centromere defects

The fragile sites observed on *X. borealis* chromosomes were reminiscent of secondary constrictions that occur at repetitive, late-replicating regions such as ribosomal DNA (rDNA).[47,49] In *Xenopus*, the rDNA transcription machinery associates with mitotic chromosomes early in development and in egg extract,[50–53] even though rDNA transcription and nucleolus formation occur after zygotic genome activation.[54,55] We therefore tested whether ultra-thin regions of *X. borealis* chromosomes replicated in *X. tropicalis* extract contained rDNA by performing immunofluorescence using antibodies against RNA polymerase I (RNA Pol I) and the rDNA transcription regulator upstream binding factor (UBF). Both proteins were consistently enriched on the ultra-thin regions of *X. borealis* mitotic chromosomes assembled in *X. tropicalis* egg extract (Figures 5A and 5B).

To test whether RNA Pol I occupancy at rDNA of *X. borealis* chromosomes contributed to the observed defects, *X. tropicalis* extract reactions were treated with the inhibitor BMH-21, which has been shown to dissociate the polymerase from chromatin.[56,57] Strikingly, *X. borealis* chromosome morphology defects as well as CENP-A localization were rescued (Figures 5C and 5D). Interestingly, further analysis of CENP-A ChIP-seq reads revealed that, in contrast to other repetitive elements, rRNA and snRNA are specifically associated with *X. borealis* centromeres, showing a distinct enrichment not observed in *X. laevis* and *X. tropicalis* (Figure S5A). Together, these data suggest that the replication stress experienced by *X. borealis* mitotic chromosomes occurs at rDNA loci, and that defects in rDNA chromatin dynamics act to destabilize a subset of *X. borealis* centromeres. In contrast, centromere formation on *X. laevis* chromosomes was not rescued by RNA Pol I inhibition (Figures S5B and S5C), further indicating differences in the mechanisms underlying their incompatibility with *X. tropicalis*. However, we observed that inhibition of RNA Pol II with triptolide partially rescued CENP-A localization to *X. laevis* chromosomes in *X. tropicalis* extract, whereas *X. borealis* chromosomes were not affected (Figure 5E), and no species' chromosomes were rescued by inhibition of RNA Pol III (Figures S5D and S5E). Therefore, a common theme in hybrid incompatibility among *Xenopus* species may be replication-transcription conflicts that contribute to eviction of CENP-A from a subset of mitotic chromosomes. However, whereas this occurs at rDNA on *X. borealis* chromosomes and depends on RNA Pol I, *X. laevis* defects may be driven, at least in part, by RNA Pol II-induced defects. These observations lead to the model that epigenetic mechanisms promoting CENP-A incorporation at centromeres are disrupted by the presence or activity of RNA polymerases that cause under-replication at specific chromosome loci. Whereas *X. laevis* defects can be overcome by driving CENP-A incorporation at centromeres, *X. borealis* defects can only be rescued by blocking replication stress at rDNA, either by preventing fork collapse or by removing RNA Pol I.

Chromosome mis-segregation can be reduced in hybrid embryos, but inviability persists

To determine whether the incompatibility mechanisms identified through this work are responsible for hybrid inviability *in vivo*, we performed rescue experiments on cross-fertilized embryos. *In vitro*-translated, paternally matched CENP-A and HJURP proteins were microinjected into both blastomeres of the two-cell hybrid embryo produced by fertilizing *X. tropicalis* eggs with *X. laevis* sperm, while *X. tropicalis* egg/*X. borealis* sperm hybrid embryos were treated with RNA Pol I inhibitor BMH-21. Fewer micronuclei were observed in both cases, indicating a decrease in mitotic errors in hybrid embryos, although not to the low levels seen in wild-type *X. tropicalis* embryos (Figures 6A and S6). Thus, the basis of chromosome defects identified using our *in vitro* egg extract assays also contribute to chromosome segregation defects *in vivo*. However, despite this partial rescue, treated hybrids died at the same time and in the same manner as untreated sibling controls (Figures 6B and 6C; Videos S1 and S2). While it is possible that a complete rescue of chromosome segregation defects in the hybrid embryos is required for viability, we predict that other mechanisms that we have not yet identified also

CellPress
OPEN ACCESS

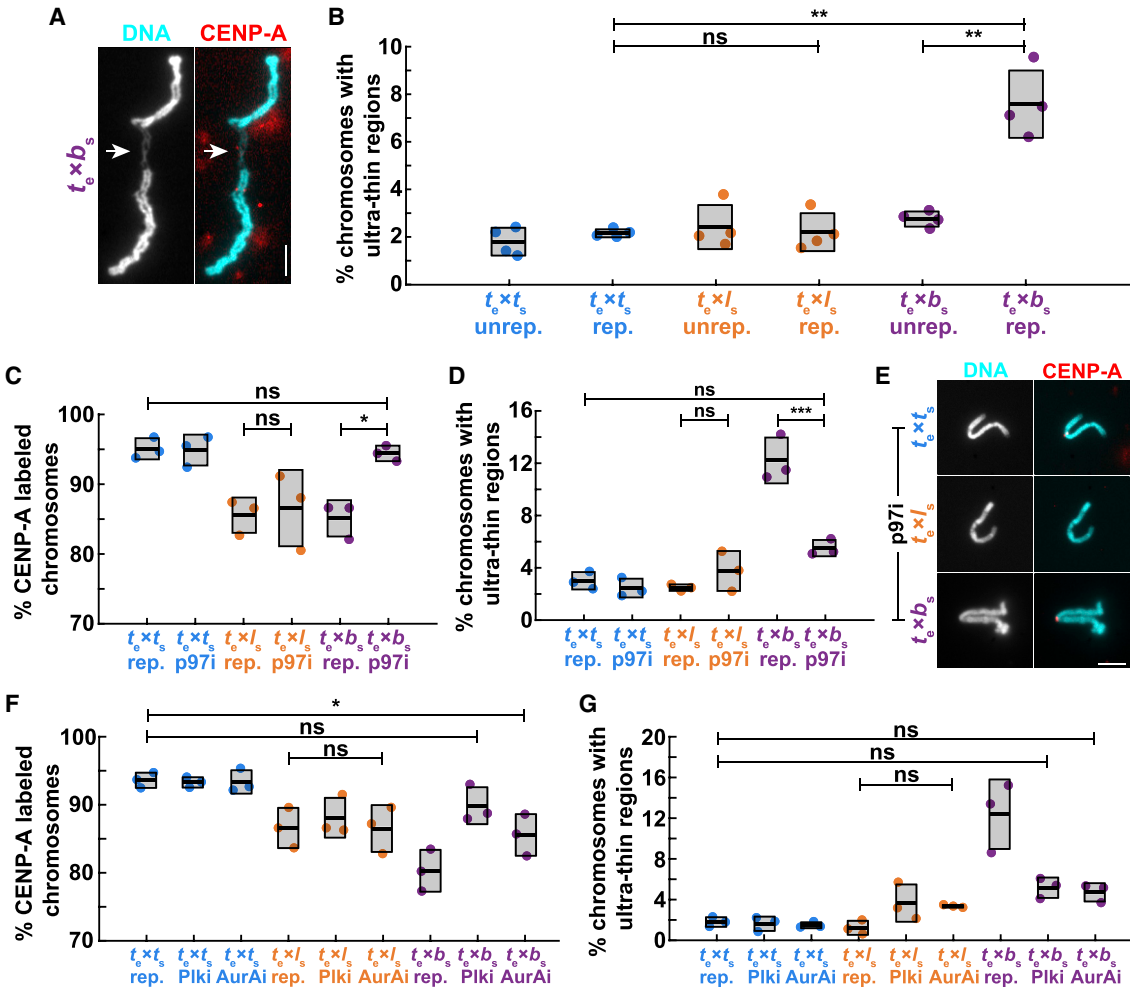

Figure 4. Mitotic replication stress leads to *X. borealis* centromere and chromosome morphology defects

(A) Representative image showing an ultra-thin region of a mitotic *X. borealis* chromosome formed in *X. tropicalis* egg extract. Note that the chromosome has an intact centromere. DNA in cyan, CENP-A in red. Scale bar, 5 μm.

(B) Percentage of unreplicated and replicated mitotic chromosomes with ultra-thin morphology defects in *X. tropicalis* extract. A low percentage of *X. tropicalis*, *X. laevis*, or *X. borealis* unreplicated chromosomes display ultra-thin regions. After cycling through interphase, only *X. borealis* chromosomes exhibit a significant increase in this defect. Quantification with n = 3 extracts, n > 310 chromosomes per extract. p values (top to bottom, then left to right) by one-way ANOVA with Tukey post hoc analysis: 2.9352e−7, 0.9999, and 1.6475e−6.

(C) Percentage of replicated chromosomes with centromeric CENP-A staining in *X. tropicalis* extracts treated with solvent control or 10 μM p97 ATPase inhibitor NMS-873 (p97i). Inhibition of p97 restores CENP-A staining on *X. borealis* mitotic chromosomes but does not affect *X. tropicalis* or *X. laevis* chromosomes. p values (top to bottom, then left to right) by one-way ANOVA with Tukey post hoc analysis: 0.9997, 0.9978, and 0.0204.

(D) Percentage of chromosomes with ultra-thin regions in *X. tropicalis* extracts treated with solvent control or 10-μM p97 ATPase inhibitor NMS-873 (p97i). Inhibition of p97 rescues *X. borealis* chromosome morphology defects but does not affect *X. tropicalis* or *X. laevis* chromosomes. p values (top to bottom, then left to right) by one-way ANOVA with Tukey post hoc analysis: 0.1114, 0.6903, and 6.2572e−5.

(E) Representative images of mitotic replicated *X. tropicalis*, *X. laevis*, and *X. borealis* chromosomes following treatment with 10-μM p97 ATPase inhibitor NMS-873 (p97i). *X. borealis* chromosome morphology and centromere localization are rescued (bottom panels, compare with Figures 2B and 4A), similar to *X. tropicalis*, while *X. laevis* chromosomes have lost CENP-A staining (middle panels). DNA in cyan, CENP-A in red. Scale bar, 5 μm.

(F) Percentage of replicated chromosomes with centromeric CENP-A staining in *X. tropicalis* extracts treated with solvent control, 1-μM Polo-like kinase 1 inhibitor BI-2536 (Plk1i), or 1-μM aurora A kinase inhibitor MLN-8237 (AurAi). CENP-A localization is fully or partially rescued on *X. borealis* mitotic chromosomes, whereas *X. tropicalis* or *X. laevis* chromosomes are not affected. p values (top to bottom) by one-way ANOVA with Tukey post hoc analysis: 0.0276, 0.7003, and 0.9999.

(G) Percentage of chromosomes with ultra-thin regions in *X. tropicalis* extracts treated with solvent control, 1-μM Polo-like kinase 1 inhibitor BI-2536 (Plk1i), or 1-μM Aurora A kinase inhibitor MLN-8237 (AurAi). Inhibition of Plk1 and AurA rescued *X. borealis* mitotic chromosome morphology defects but did not affect *X. tropicalis* or *X. laevis* chromosomes. p values (top to bottom) by one-way ANOVA with Tukey post hoc analysis: 0.2882, 0.1525, and 0.5887.

(C and D) n = 3 extracts, n > 179 chromosomes per extract.

(E and F) n = 3 extracts, n > 155 chromosomes per extract.

(B–F) ns, not significant.

See also Figure S4.

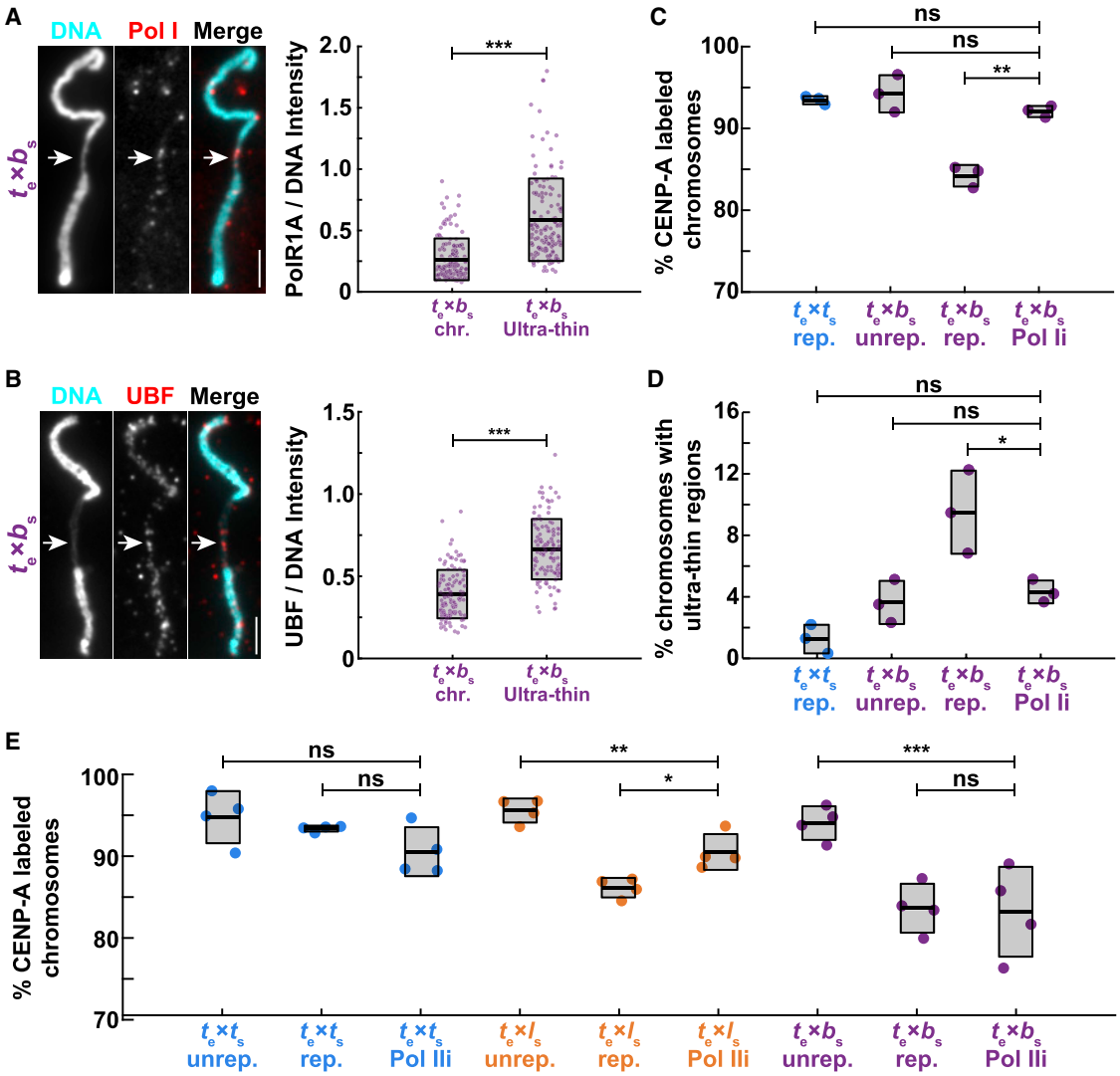

Figure 5. Replication-transcription conflicts at rDNA on *X. borealis* chromosomes can be rescued by inhibiting RNA Pol I

(A) Representative images and fluorescence intensity quantification of RNA Pol I staining relative to DNA on ultra-thin and normal regions of *X. borealis* mitotic chromosomes, revealing enrichment of RNA Pol I on ultra-thin regions. Quantification with n = 3 extracts, n = 140 chromosomes. p value = 9.4793e−20 by two-tailed two-sample unequal variance t tests.

(B) Representative images and fluorescence intensity quantification of UBF staining relative to DNA on ultra-thin and normal regions of *X. borealis* mitotic chromosomes, revealing enrichment of UBF on ultra-thin regions. Quantification with n = 3 extracts, n = 62 chromosomes. p value = 4.5004e−13 by two-tailed two-sample unequal variance t tests.

(C) Percentage of mitotic chromosomes with centromeric CENP-A staining in *X. tropicalis* extracts treated with solvent control or 1-μM BMH-21 to inhibit RNA Pol I (Pol Ii), which fully rescues CENP-A localization on replicated *X. borealis* chromosomes. p values (top to bottom) by one-way ANOVA with Tukey post hoc analysis: 0.9794, 0.7979, and 0.0005.

(D) Percentage of mitotic chromosomes with ultra-thin regions in *X. tropicalis* extracts treated with solvent control or 1-μM BMH-21 (Pol Ii). RNA Pol I inhibition also rescues *X. borealis* chromosome morphology defects. p values (top to bottom) by one-way ANOVA with Tukey post hoc analysis: 0.5078, 0.9999, and 0.0469.

(E) Percentage of chromosomes with centromeric CENP-A staining in *X. tropicalis* extracts treated with solvent control or 25-μM triptolide to inhibit RNA Pol II (RNA Pol IIi). *X. laevis* chromosomes are partially rescued, while *X. tropicalis* and *X. borealis* chromosomes are not affected. Quantification with n = 3 extracts, n > 322 chromosomes per extract. p values (top to bottom, then left to right) by one-way ANOVA with Tukey post hoc analysis: 0.4785, 0.8797, 0.0052, 0.0125, 0.0003, and 0.9999.

(A and B) DNA in cyan, RNA Pol I and UBF in red. Scale bars, 5 μm.

(C and D) n = 3 extracts, n > 172 chromosomes per extract.

(C–E) ns, not significant.

See also Figure S5.

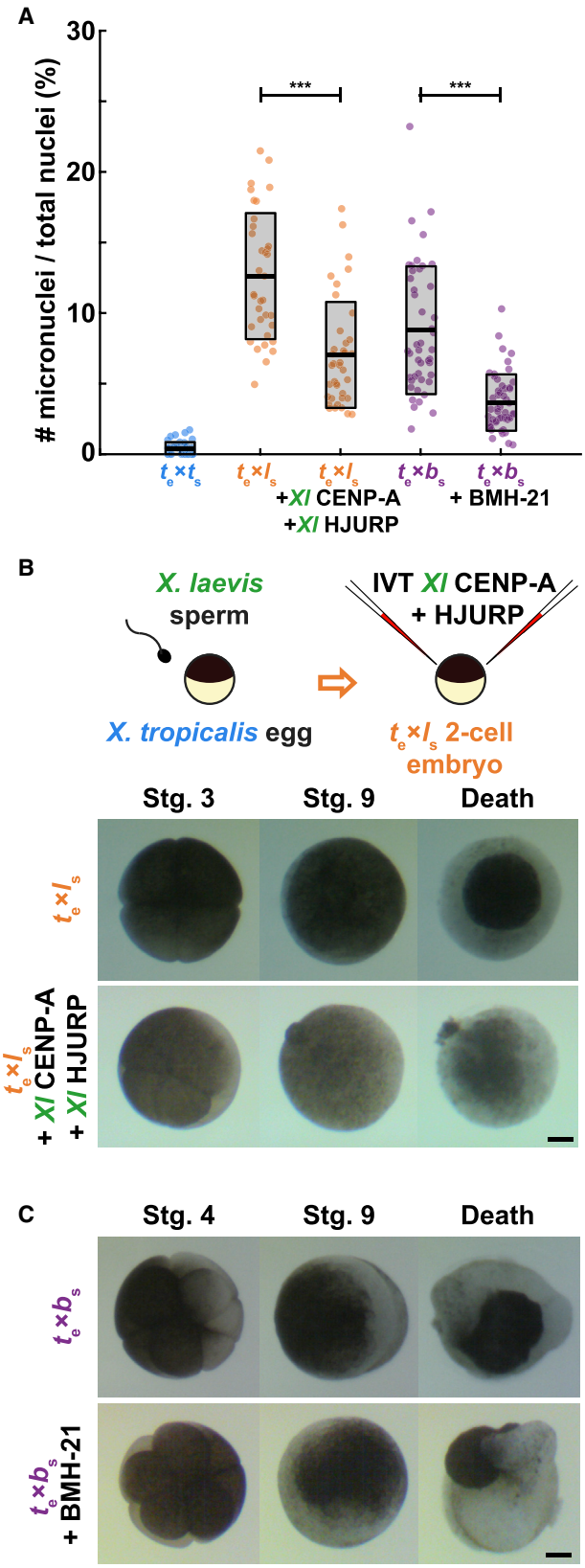

Figure 6. Treatments that rescue CENP-A localization in egg extracts reduce micronuclei formation in hybrid embryos, but inviability persists

(A) Quantification of chromosome mis-segregation events as measured by the number of micronuclei compared with total nuclei in treated hybrid embryos. *X. tropicalis* eggs fertilized with *X. laevis* sperm were microinjected with *X. laevis* CENP-A/HJURP, while *X. tropicalis* eggs fertilized with *X. borealis* sperm were treated with RNA Pol I inhibitor BMH-21. Embryos were fixed at stage 9 (7 hpf) just before gastrulation and hybrid death. The number of micronuclei was significantly reduced in both cases, but not to control levels measured in *X. tropicalis* eggs fertilized with *X. tropicalis* sperm. n = 3 clutches for each hybrid, n > 15 embryos and > 200 cells per embryo. p values (left to right) by two-tailed two-sample unequal variance t tests: 2.111e−7 and 2.651e−9; ns, not significant.

(B) Schematic of experiment and video frames of *X. tropicalis* eggs fertilized with *X. laevis* sperm microinjected at the two-cell stage with *X. laevis* CENP-A/HJURP, increasing centromeric protein concentration by ~44.5%. Microinjected hybrid embryos die at the same time and in the same manner as uninjected hybrid controls. n = 10 embryos across 4 clutches. Scale bar, 200 μm. See also Video S1.

(C) Video frames of *X. tropicalis* eggs fertilized with *X. borealis* sperm that were incubated from the two-cell stage with 1-μM RNA Pol I inhibitor, BMH-21. Treated hybrid embryos die at the same time and in the same manner as untreated hybrid controls. n = 12 embryos across 2 clutches. Scale bar, 200 μm. See also Video S2.

See also Figure S6.

contribute, which can be uniquely addressed using a combination of *in vitro* and *in vivo* approaches in *Xenopus*.

DISCUSSION

Centromeric DNA sequences and centromere and kinetochore proteins have been shown to rapidly co-evolve, which is thought to counteract female meiotic drive and maintain faithful chromosome segregation.[5,36,58–60] Our study reveals very low conservation of core centromere DNA sequences across three *Xenopus* species, and differences in protein sequences of *Xenopus* CENP-A and its chaperone HJURP are also observed. However, robust epigenetic mechanisms must operate to maintain centromere compatibility in *Xenopus* hybrids, since many crosses are viable,[24,61–63] and only a subset of chromosomes display centromere/kinetochore defects in inviable hybrids.[25] Thus, neither differences in centromere sequences nor centromere/kinetochore proteins appear to contribute directly to *Xenopus* hybrid inviability, although more detailed analysis of *X. borealis* centromeres will be necessary to fully address this point.

The *Xenopus* egg extract and sperm chromosome reconstitution system uniquely allowed us to identify mechanisms by which centromere formation is disrupted on specific chromosomes in inviable interspecies hybrids. For *X. tropicalis* eggs fertilized with *X. borealis* sperm, *in vitro* experiments indicate that defects result from replication stress at rDNA, since both CENP-A localization and chromosome morphology can be rescued by either evicting RNA Pol I or preventing replication fork collapse by inhibiting the chaperone p97.[45,50,53] However, it is unclear why distinct subsets of paternal chromosomes appear to possess ultra-thin regions versus centromere defects. Given the observed enrichment of rRNA and snRNA repeats associated with *X. borealis* centromeres, we propose that clustering of repetitive elements including rDNA, pericentromeric, and centromeric repeats during interphase brings together different

chromosomal loci and their associated machineries. Normally, such clustering is observed at chromocenters, which may function to stabilize centromeres and promote CENP-A deposition in early G1 of the cell cycle.[64,65] Although discrete chromocenters or other nuclear bodies such as nucleoli have not been observed to form in egg extracts, hybrid reactions may be revealing *trans* interactions that normally occur during interphase across rDNA loci, including the centromere-adjacent regions of four specific *X. borealis* chromosomes. Intriguingly, the p97 chaperone has been implicated in both CENP-A extraction from centromeres and activation of rDNA transcription in *Arabidopsis*.[66] While addition of excess CENP-A and its chaperone HJURP can rescue centromere assembly on these chromosomes during interphase, we propose that incomplete rDNA replication at the onset of mitosis due to RNA Pol I occupancy and/or transcription locally recruits p97, which causes both fork collapse and CENP-A extraction from neighboring centromeres. Understanding how formation of fragile sites and centromere loss are related will require a complete *X. borealis* genome assembly that includes rDNA and other repetitive sequences.

Our findings highlight the dynamic interplay between machineries that promote and disrupt centromere assembly. For *in vitro* reactions reconstituting *X. tropicalis* eggs fertilized with *X. laevis* sperm, the disruption does not involve RNA Pol I or replication stress. Centromere defects appear less severe in this hybrid reaction and can be fully rescued by addition of either species-matched or overexpressed CENP-A/HJURP and partially rescued by RNA Pol II eviction, treatments that may reinforce epigenetic machineries that maintain centromeres. Thus, distinct mechanisms underlie centromere disruption in the two inviable hybrids, but defects in both cases are consistent with observations that aberrant polymerase occupancy or transcription adjacent to a centromere can compromise its assembly.[67–69]

An open question is how the incompatibilities we have characterized *in vitro* manifest in hybrid embryos *in vivo*. Whole-genome sequencing of the *X. tropicalis* egg/*X. laevis* sperm hybrid just prior to embryo death combined with preliminary Hi-C analysis indicates that the long arms of chromosomes 3L and 4L have been largely eliminated, but the centromere persists on the short arm allowing it to be retained[25] (unpublished data). One possible explanation is that under-replication of repetitive sequences adjacent to the centromere in this hybrid initially disrupts centromere assembly, but after chromosome breakage, the adjacent, troublesome sequences are removed, and the centromere stabilizes on the short arm while the long arm lacking the centromere frequently ends up in micronuclei and is eventually degraded. Because micronuclei are observed throughout embryogenesis in both inviable hybrids,[25] multiple rounds of chromosome mis-segregation and instability likely occur that give rise to the terminal karyotype. In the *X. tropicalis* egg/*X. borealis* sperm inviable hybrid that experiences replication stress, a pathway involving p97-mediated extraction and degradation of the replicative helicase that leads to fork breakage and microhomology-mediated end joining events likely operates, which has been well characterized in *Xenopus* egg extracts.[45] Detailed genomic analysis of chromosome deletions and rearrangements in hybrid embryos will shed light on how replication-transcription conflicts give rise to specific chromosome defects, while additional *in vitro* experiments will reveal underlying molecular mechanisms.

Death of inviable *Xenopus* hybrids occurs at gastrulation when the zygotic genome undergoes widespread transcriptional activation, and the distinct death phenotypes observed upon fertilization of *X. tropicalis* eggs with either *X. laevis* or *X. borealis* sperm may be due to the different sets of genes affected by the loss of specific chromosomal loci. However, despite a reduction in micronuclei upon hybrid embryo treatments that rescued centromere formation *in vitro*, death was not delayed, or the phenotypes altered in any way. Therefore, we hypothesize that other incompatibilities also contribute to hybrid inviability. In particular, mismatches between mitochondrial and nuclear-encoded genes have been shown to underlie inviability in some hybrids.[70,71]

In conclusion, our findings identify defects in epigenetic centromere maintenance that contribute to hybrid inviability. The combination of *in vivo*, *in vitro*, and genomic approaches possible in *Xenopus* promise to provide further mechanistic insights into the molecular basis of hybrid fates and speciation.

STAR★METHODS

Detailed methods are provided in the online version of this paper and include the following:

- KEY RESOURCES TABLE
- RESOURCE AVAILABILITY
  - Lead contact
  - Materials availability
  - Data and code availability
- EXPERIMENTAL MODEL AND SUBJECT DETAILS
  - Chemicals
  - Frog care
- METHOD DETAILS
  - CENP-A ChIP-seq and data analysis
  - Protein sequence alignments
  - *Xenopus* egg extracts
  - Chromosome immunofluorescence
  - Nuclear DNA FISH for FCR centromeric sequences
  - Protein expression in reticulocyte lysate
  - Western blots
  - Drug treatments
  - Chromosome and nuclei imaging
  - In vitro fertilization and cross-fertilizations
  - Embryo microinjection
  - Embryo video imaging
  - Embryo whole-mount immunofluorescence
  - Confocal microscopy
- QUANTIFICATION AND STATISTICAL ANALYSIS

SUPPLEMENTAL INFORMATION

Supplemental information can be found online at https://doi.org/10.1016/j.cub.2022.07.037.

ACKNOWLEDGMENTS

We thank Daniel Rokshar, Austin Mudd, Sofia Medina-Ruiz, and Mariko Kondo for early access to *X. borealis* CENP-A, CENP-C, HJURP, and H3 sequences.

We also thank students Elizabeth Turcotte, Costa Bartolutti, Justin Peng, and Christian Erikson for help with experiments to M.K. We are grateful to the Welch, King, Dernberg, Karpen, Lewis, and Rokshar laboratories at UC Berkeley for sharing reagents, discussions, and expertise. We thank all past and present members of the Heald laboratory, Coral Y. Zhou, Gary Karpen, Dirk Hockemeyer, Rasmus Nielsen, and Mark J. Khoury for continuous support and fruitful discussions. M.K. was supported by a National Science Foundation (NSF) GRFP fellowship. O.K.S. was supported by a National Institutes of Health (NIH) T32 GM113854-02 and an NSF GRFP fellowship. A.F.S. was supported by NIH NIGMS R01 GM074728. R.H. was supported by NIH MIRA grant R35 GM118183 and the Flora Lamson Hewlett Chair.

AUTHOR CONTRIBUTIONS

Conceptualization and funding acquisition, R.H. and M.K.; methodology, investigation, and visualization, M.K. and O.K.S.; supervision, A.F.S. and R.H.; manuscript preparation, M.K., R.H., O.K.S., and A.F.S.

DECLARATION OF INTERESTS

The authors declare no competing interests.

Received: March 7, 2022
Revised: June 15, 2022
Accepted: July 15, 2022
Published: August 15, 2022

REFERENCES

1. Sanei, M., Pickering, R., Kumke, K., Nasuda, S., and Houben, A. (2011). Loss of centromeric histone H3 (CENH3) from centromeres precedes uniparental chromosome elimination in interspecific barley hybirds. Proc. Natl. Acad. Sci. USA *108*, E498–E505.
2. Maheshwari, S., and Barbash, D.A. (2011). The genetics of hybrid incompatibilities. Annu. Rev. Genet. *45*, 331–355.
3. Fujiwara, A., Abe, S., Yamaha, E., Yamazaki, F., and Yoshida, M.C. (1997). Uniparental chromosome elimination in the early embryogenesis of the inviable salmonid hybrids between masu salmon female and rainbow trout male. Chromosoma *106*, 44–52.
4. Gernand, D., Rutten, T., Varshney, A., Rubtsova, M., Prodanovic, S., Brüss, C., Kumlehn, J., Matzk, F., and Houben, A. (2005). Uniparental chromosome elimination at mitosis and interphase in wheat and pearl millet crosses involves micronucleus formation, progressive heterochromatinization, and DNA fragmentation. Plant Cell *17*, 2431–2438.
5. Malik, H.S., and Henikoff, S. (2001). Adaptive evolution of Cid, a centromere-specific histone in *Drosophila*. Genetics *157*, 1293–1298.
6. Maheshwari, S., Tan, E.H., West, A., Franklin, F.C.H., Comai, L., and Chan, S.W.L. (2015). Naturally occurring differences in CENH3 affect chromosome segregation in zygotic mitosis of hybrids. PLoS Genet. *11*, e1004970.
7. Rosin, L., and Mellone, B.G. (2016). Co-evolving CENP-A and CAL1 domains mediate centromeric CENP-A deposition across *Drosophila* species. Dev. Cell *37*, 136–147.
8. Pentakota, S., Zhou, K., Smith, C., Maffini, S., Petrovic, A., Morgan, G.P., Weir, J.R., Vetter, I.R., Musacchio, A., and Luger, K. (2017). Decoding the centromeric nucleosome through CENP-N. eLife *6*, e33442.
9. Chittori, S., Hong, J., Saunders, H., Feng, H., Ghirlando, R., Kelly, A.E., Bai, Y., and Subramaniam, S. (2018). Structural mechanisms of centromeric nucleosome recognition by the kinetochore protein CENP-N. Science *359*, 339–343.
10. Tian, T., Li, X., Liu, Y., Wang, C., Liu, X., Bi, G., Zhang, X., Yao, X., Zhou, Z.H., and Zang, J. (2018). Molecular basis for CENP-N recognition of CENP-A nucleosome on the human kinetochore. Cell Res. *28*, 374–378.
11. Falk, S.J., Guo, L.Y., Sekulic, N., Smoak, E.M., Mani, T., Logsdon, G.A., Gupta, K., Jansen, L.E.T., Van Duyne, G.D., Vinogradov, S.A., et al. (2015). Chromosomes. CENP-C reshapes and stabilizes CENP-A nucleosomes at the centromere. Science *348*, 699–703.
12. French, B.T., Westhorpe, F.G., Limouse, C., and Straight, A.F. (2017). *Xenopus laevis* M18BP1 directly binds existing CENP-A nucleosomes to promote centromeric chromatin assembly. Dev. Cell *42*, 190–199.e10.
13. Shono, N., Ohzeki, J.I., Otake, K., Martins, N.M.C., Nagase, T., Kimura, H., Larionov, V., Earnshaw, W.C., and Masumoto, H. (2015). CENP-C and CENP-I are key connecting factors for kinetochore and CENP-A assembly. J. Cell Sci. *128*, 4572–4587.
14. Hori, T., Shang, W.H., Hara, M., Ariyoshi, M., Arimura, Y., Fujita, R., Kurumizaka, H., and Fukagawa, T. (2017). Association of M18BP1/KNL2 with CENP-A nucleosome is essential for centromere formation in non-mammalian vertebrates. Dev. Cell *42*, 181–189.e3.
15. Moree, B., Meyer, C.B., Fuller, C.J., and Straight, A.F. (2011). CENP-C recruits M18BP1 to centromeres to promote CENP-A chromatin assembly. J. Cell Biol. *194*, 855–871.
16. Carroll, C.W., Silva, M.C.C., Godek, K.M., Jansen, L.E.T., and Straight, A.F. (2009). Centromere assembly requires the direct recognition of CENP-A nucleosomes by CENP-N. Nat. Cell Biol. *11*, 896–902.
17. Jagannathan, M., and Yamashita, Y.M. (2021). Defective satellite DNA clustering into chromocenters underlies hybrid incompatibility in *Drosophila*. Mol. Biol. Evol. *38*, 4977–4986.
18. Thomae, A.W., Schade, G.O.M., Padeken, J., Borath, M., Vetter, I., Kremmer, E., Heun, P., and Imhof, A. (2013). A pair of centromeric proteins mediates reproductive isolation in *Drosophila* species. Dev. Cell *27*, 412–424.
19. Satyaki, P.R.V., Cuykendall, T.N., Wei, K.H.C., Brideau, N.J., Kwak, H., Aruna, S., Ferree, P.M., Ji, S., and Barbash, D.A. (2014). The Hmr and Lhr hybrid incompatibility genes suppress a broad range of heterochromatic repeats. PLoS Genet. *10*, e1004240.
20. Anselm, E., Thomae, A.W., Jeyaprakash, A.A., and Heun, P. (2018). Oligomerization of Drosophila nucleoplasmin-Like Protein is required for its centromere localization. Nucleic Acids Res. *46*, 11274–11286.
21. Lukacs, A., Thomae, A.W., Krueger, P., Schauer, T., Venkatasubramani, A.V., Kochanova, N.Y., Aftab, W., Choudhury, R., Forne, I., and Imhof, A. (2021). The integrity of the HMR complex is necessary for centromeric binding and reproductive isolation in *Drosophila*. PLoS Genet. *17*, e1009744.
22. Blum, J.A., Bonaccorsi, S., Marzullo, M., Palumbo, V., Yamashita, Y.M., Barbash, D.A., and Gatti, M. (2017). The hybrid incompatibility genes Lhr and Hmr are required for sister chromatid detachment during anaphase but not for centromere function. Genetics *207*, 1457–1472.
23. Session, A.M., Uno, Y., Kwon, T., Chapman, J.A., Toyoda, A., Takahashi, S., Fukui, A., Hikosaka, A., Suzuki, A., Kondo, M., et al. (2016). Genome evolution in the allotetraploid frog *Xenopus laevis*. Nature *538*, 336–343.
24. Narbonne, P., Simpson, D.E., and Gurdon, J.B. (2011). Deficient induction response in a Xenopus nucleocytoplasmic hybrid. PLoS Biol. *9*, e1001197.
25. Gibeaux, R., Acker, R., Kitaoka, M., Georgiou, G., van Kruijsbergen, I., Ford, B., Marcotte, E.M., Nomura, D.K., Kwon, T., Veenstra, G.J.C., et al. (2018). Paternal chromosome loss and metabolic crisis contribute to hybrid inviability in Xenopus. Nature *553*, 337–341.
26. Smith, O.K., Limouse, C., Fryer, K.A., Teran, N.A., Sundararajan, K., Heald, R., and Straight, A.F. (2021). Identification and characterization of centromeric sequences in *Xenopus laevis*. Genome Res. *31*, 958–967.
27. McKinley, K.L., and Cheeseman, I.M. (2016). The molecular basis for centromere identity and function. Nat. Rev. Mol. Cell Biol. *17*, 16–29.
28. Westhorpe, F.G., and Straight, A.F. (2014). The centromere: epigenetic control of chromosome segregation during mitosis. Cold Spring Harb. Perspect. Biol. *7*, a015818.
29. Panchenko, T., and Black, B.E. (2009). The epigenetic basis for centromere identity. Prog. Mol. Subcell. Biol. *48*, 1–32.
30. Foltz, D.R., Jansen, L.E.T., Bailey, A.O., Yates, J.R., Bassett, E.A., Wood, S., Black, B.E., and Cleveland, D.W. (2009). Centromere-specific assembly of CENP-A nucleosomes is mediated by HJURP. Cell *137*, 472–484.

31. Dunleavy, E.M., Roche, D., Tagami, H., Lacoste, N., Ray-Gallet, D., Nakamura, Y., Daigo, Y., Nakatani, Y., and Almouzni-Pettinotti, G. (2009). HJURP is a cell-cycle-dependent maintenance and deposition factor of CENP-A at centromeres. Cell *137*, 485–497.

32. Hu, H., Liu, Y., Wang, M., Fang, J., Huang, H., Yang, N., Li, Y., Wang, J., Yao, X., Shi, Y., et al. (2011). Structure of a CENP-A-histone H4 heterodimer in complex with chaperone HJURP. Genes Dev. *25*, 901–906.

33. Rosin, L.F., and Mellone, B.G. (2017). Centromeres drive a hard bargain. Trends Genet. *33*, 101–117.

34. Henikoff, S., Ahmad, K., and Malik, H.S. (2001). The centromere paradox: stable inheritance with rapidly evolving DNA. Science *293*, 1098–1102.

35. Malik, H.S., and Henikoff, S. (2009). Major evolutionary transitions in centromere complexity. Cell *138*, 1067–1082.

36. Kumon, T., Ma, J., Akins, R.B., Stefanik, D., Nordgren, C.E., Kim, J., Levine, M.T., and Lampson, M.A. (2021). Parallel pathways for recruiting effector proteins determine centromere drive and suppression. Cell *184*, 4904–4918.e11.

37. Maresca, T.J., and Heald, R. (2006). Methods for studying spindle assembly and chromosome condensation in Xenopus egg extracts. Methods Mol. Biol. *322*, 459–474.

38. French, B.T., and Straight, A.F. (2017). The power of Xenopus egg extract for reconstitution of centromeres and kinetochore function. Prog. Mol. Subcell. Biol. *56*, 59–84.

39. Bernad, R., Sánchez, P., Rivera, T., Rodríguez-Corsino, M., Boyarchuk, E., Vassias, I., Ray-Gallet, D., Arnaoutov, A., Dasso, M., Almouzni, G., et al. (2011). Xenopus HJURP and condensin II are required for CENP-A assembly. J. Cell Biol. *192*, 569–582.

40. Milks, K.J., Moree, B., and Straight, A.F. (2009). Dissection of CENP-C—directed Centromere and Kinetochore Assembly. Mol. Biol. Cell *20*, 4246–4255.

41. Zasadzińska, E., Huang, J., Bailey, A.O., Guo, L.Y., Lee, N.S., Srivastava, S., Wong, K.A., French, B.T., Black, B.E., and Foltz, D.R. (2018). Inheritance of CENP-A nucleosomes during DNA replication requires HJURP. Dev. Cell *47*, 348–362.e7.

42. Erhardt, S., Mellone, B.G., Betts, C.M., Zhang, W., Karpen, G.H., and Straight, A.F. (2008). Genome-wide analysis reveals a cell cycle-dependent mechanism controlling centromere propagation. J. Cell Biol. *183*, 805–818.

43. Roure, V., Medina-Pritchard, B., Lazou, V., Rago, L., Anselm, E., Venegas, D., Jeyaprakash, A.A., and Heun, P. (2019). Reconstituting drosophila centromere identity in human cells. Cell Rep. *29*, 464–479.e5.

44. Gómez-González, B., and Aguilera, A. (2019). Transcription-mediated replication hindrance: a major driver of genome instability. Genes Dev. *33*, 1008–1026.

45. Deng, L., Wu, R.A., Sonneville, R., Kochenova, O.V., Labib, K., Pellman, D., and Walter, J.C. (2019). Mitotic CDK promotes replisome disassembly, fork breakage, and complex DNA rearrangements. Mol. Cell *73*, 915–929.e6.

46. Kabeche, L., Nguyen, H.D., Buisson, R., and Zou, L. (2018). A mitosis-specific and R loop-driven ATR pathway promotes faithful chromosome segregation SUPP. Science *359*, 108–114.

47. Durkin, S.G., and Glover, T.W. (2007). Chromosome fragile sites. Annu. Rev. Genet. *41*, 169–192.

48. Maric, M., Maculins, T., De Piccoli, G., and Labib, K. (2014). Cdc48 and a ubiquitin ligase drive disassembly of the CMG helicase at the end of DNA replication. Science *346*, 1253596.

49. Durica, D.S., and Krider, H.M. (1977). Studies on the ribosomal RNA cistrons in interspecific Drosophila hybrids. I. Nucleolar dominance. Dev. Biol. *59*, 62–74.

50. Roussel, P., André, C., Comai, L., and Hernandez-Verdun, D. (1996). The rDNA transcription machinery is assembled during mitosis in active NORs and absent in inactive NORs. J. Cell Biol. *133*, 235–246.

51. Gébrane-Younès, J., Fomproix, N., and Hernandez-Verdun, D. (1997). When rDNA transcription is arrested during mitosis, UBF is still associated with non-condensed rDNA. J. Cell Sci. *110*, 2429–2440.

52. Bell, P., and Scheer, U. (1997). Prenucleolar bodies contain coilin and are assembled in Xenopus egg extract depleted of specific nucleolar proteins and U3 RNA. J. Cell Sci. *110*, 43–54.

53. Bell, P., Mais, C., McStay, B., and Scheer, U. (1997). Association of the nucleolar transcription factor UBF with the transcriptionally inactive rRNA genes of pronuclei and early Xenopus embryos. J. Cell Sci. *110*, 2053–2063.

54. Shiokawa, K., Kurashima, R., and Shinga, J. (1994). Temporal control of gene expression from endogenous and exogenously- introduced DNAs in early embryogenesis of *Xenopus laevis*. Int. J. Dev. Biol. *38*, 249–255.

55. Newport, J., and Kirschner, M. (1982). A major developmental transition in early Xenopus embryos: I. characterization and timing of cellular changes at the midblastula stage. Cell *30*, 675–686.

56. Peltonen, K., Colis, L., Liu, H., Trivedi, R., Moubarek, M.S., Moore, H.M., Bai, B., Rudek, M.A., Bieberich, C.J., and Laiho, M. (2014). A targeting modality for destruction of RNA polymerase I that possesses anticancer activity. Cancer Cell *25*, 77–90.

57. Colis, L., Peltonen, K., Sirajuddin, P., Liu, H., Sanders, S., Ernst, G., Barrow, J.C., and Laiho, M. (2014). DNA intercalator BMH-21 inhibits RNA polymerase I independent of DNA damage response. Oncotarget *5*, 4361–4369.

58. Malik, H.S., Vermaak, D., and Henikoff, S. (2002). Recurrent evolution of DNA-binding motifs in the Drosophila centromeric histone. Proc. Natl. Acad. Sci. USA *99*, 1449–1454.

59. Pontremoli, C., Forni, D., Pozzoli, U., Clerici, M., Cagliani, R., and Sironi, M. (2021). Kinetochore proteins and microtubule-destabilizing factors are fast evolving in eutherian mammals. Mol. Ecol. *30*, 1505–1515.

60. van Hooff, J.J., Tromer, E., van Wijk, L.M., Snel, B., and Kops, G.J. (2017). Evolutionary dynamics of the kinetochore network in eukaryotes as revealed by comparative genomics. EMBO Rep. *18*, 1559–1571.

61. De Robertis, E.M., and Black, P. (1979). Hybrids of Xenopus laevis and Xenopus borealis express proteins from both parents. Dev. Biol. *68*, 334–339.

62. Woodland, H.R., and Ballantine, J.E.M. (1980). Paternal gene expression in developing hybrid embryos of Xenopus laevis and Xenopus borealis. J. Embryol. Exp. Morphol. *60*, 359–372.

63. Bürki, E. (1985). The expression of creatine kinase isozymes in Xenopus tropicalis, Xenopus laevis laevis, and their viable hybrid. Biochem. Genet. *23*, 73–88.

64. Brändle, F., Frühbauer, B., and Jagannathan, M. (2022). Principles and functions of pericentromeric satellite DNA clustering into chromocenters. Semin. Cell Dev. Biol. *128*, 26–39.

65. Stellfox, M.E., Bailey, A.O., and Foltz, D.R. (2013). Putting CENP-A in its place. Cell. Mol. Life Sci. *70*, 387–406.

66. Mérai, Z., Chumak, N., García-Aguilar, M., Hsieh, T.F., Nishimura, T., Schoft, V.K., Bindics, J., Slusarz, L., Arnoux, S., Opravil, S., et al. (2014). The AAA-ATPase molecular chaperone Cdc48/p97 disassembles SUMOylated centromeres, decondenses heterochromatin, and activates ribosomal RNA genes. Proc. Natl. Acad. Sci. USA *111*, 16166–16171.

67. Rošić, S., Köhler, F., and Erhardt, S. (2014). Repetitive centromeric satellite RNA is essential for kinetochore formation and cell division. J. Cell Biol. *207*, 335–349.

68. Grenfell, A.W., Heald, R., and Strzelecka, M. (2016). Mitotic noncoding RNA processing promotes kinetochore and spindle assembly in Xenopus. J. Cell Biol. *214*, 133–141.

69. Bobkov, G.O.M., Gilbert, N., and Heun, P. (2018). Centromere transcription allows CENP-A to transit from chromatin association to stable incorporation. J. Cell Biol. *217*, 1957–1972.

70. Lee, H.Y., Chou, J.Y., Cheong, L., Chang, N.H., Yang, S.Y., and Leu, J.Y. (2008). Incompatibility of nuclear and mitochondrial genomes causes hybrid sterility between two yeast species. Cell *135*, 1065–1073.

71. Ma, H., Marti Gutierrez, N., Morey, R., Van Dyken, C., Kang, E., Hayama, T., Lee, Y., Li, Y., Tippner-Hedges, R., Wolf, D.P., et al. (2016). Incompatibility between nuclear and mitochondrial genomes contributes to an interspecies reproductive barrier. Cell Metab. *24*, 283–294.

72. Bredeson, J.V., Mudd, A.B., Medina-Ruiz, S., Mitros, T., Smith, O.K., Miller, K.E., Lyons, J.B., Batra, S.S., Park, J., Berkoff, K.C., et al. (2021). Conserved chromatin and repetitive patterns reveal slow genome evolution in frogs. Preprint at bioRxiv. https://doi.org/10.1101/2021.10.18.464293.

73. Schindelin, J., Arganda-Carreras, I., Frise, E., Kaynig, V., Longair, M., Pietzsch, T., Preibisch, S., Rueden, C., Saalfeld, S., Schmid, B., et al. (2012). Fiji: an open-source platform for biological-image analysis. Nat. Methods *9*, 676–682.

74. Fu, L., Niu, B., Zhu, Z., Wu, S., and Li, W. (2012). CD-HIT: accelerated for clustering the next-generation sequencing data. Bioinformatics *28*, 3150–3152.

75. Smit, A., Hubley, R., and Green, P.. RepeatMasker Open-4.0. http://www.repeatmasker.org.

76. Kitaoka, M., Heald, R., and Gibeaux, R. (2018). Spindle assembly in egg extracts of the Marsabit clawed frog, Xenopus borealis. Cytoskeleton *75*, 244–257.

77. Hannak, E., and Heald, R. (2006). Investigating mitotic spindle assembly and function in vitro using Xenopus laevis egg extracts. Nat. Protoc. *1*, 2305–2314.

78. Brown, K.S., Blower, M.D., Maresca, T.J., Grammer, T.C., Harland, R.M., and Heald, R. (2007). Xenopus tropicalis egg extracts provide insight into scaling of the mitotic spindle. J. Cell Biol. *176*, 765–770.

79. Levy, D.L., and Heald, R. (2010). Nuclear size is regulated by importin A and Ntf2 in Xenopus. Cell *143*, 288–298.

80. Edelstein, A.D., Tsuchida, M.A., Amodaj, N., Pinkard, H., Vale, R.D., and Stuurman, N. (2014). Advanced methods of microscope control using μManager software. J. Biol. Methods *1*, 10.

81. Gibeaux, R., and Heald, R. (2019). Generation of Xenopus haploid, triploid, and hybrid embryos. Methods Mol. Biol. *1920*, 303–315.

STAR★METHODS

KEY RESOURCES TABLE

REAGENT or RESOURCE	SOURCE	IDENTIFIER
Antibodies		
Rabbit anti-xCENP-A	Straight Lab[15,40]	N/A
Rabbit anti-POLR1A	Novus Biologicals	Cat#: NBP2-56122
Mouse anti-UBTF, clone 6B6	Abnova	Cat#: H00007343-M01; RRID: AB_607269
Rabbit anti-Histone H3	Abcam	Cat#: ab1791; RRID: AB_302613
Mouse anti-Beta-tubulin E7	Developmental Studies Hybridoma Bank	Cat#: E7; RRID: AB_2315513
Mouse anti-c-myc, clone 9E10	Sigma-Aldrich	Cat#: M4439; RRID: AB_439694
Mouse anti-Ran	BD Biosciences	Cat#: 610340; RRID: AB_397730‘
Alexa Fluor 488	Invitrogen	Cat#: A-11008; RRID: AB_143165
Alexa Fluor 568	Invitrogen	Cat#: A-11011; RRID: AB_143157
Goat anti-Rabbit IgG (H&L) Antibody DyLight 800 Conjugated	Rockland Immunochemicals	Cat#: 611-145-002-0.5; RRID: AB_11183542
Donkey anti-Mouse IgG (H&L) Antibody DyLight 680 Conjugated	Rockland Immunochemicals	Cat#: 610-744-002; RRID: AB_1660920
Bacterial and virus strains		
XL1-Blue competent cells	Agilent	Cat#: 200249
Chemicals, peptides, and recombinant proteins		
Pregnant mare serum gonadotrophin	Calbiochem	Cat#: 367222
Human chorionic gonadotrophin	Sigma-Aldrich	Cat#: CG10
Hoechst 33342	Invitrogen	Cat#: H3570
Vectashield	Vector Labs	Cat#: H-1000
Alexa Fluor 568-dUTP	Invitrogen	Cat#: C11399
Random hexamers	Invitrogen	Cat#: 100026484
Klenow (exo-) polymerase	New England Biolabs	Cat#: M0212S
Blocking reagent	Roche	Cat#: 11096176001
Salmon sperm DNA	Invitrogen	Cat#: AM9680
Aphidicolin	Sigma-Aldrich	Cat#: A0781
BI-2536	Selleck Chemicals	Cat#: S1109
BMH-21	Sigma-Aldrich	Cat#: SML1183
ML-60218	Sigma-Aldrich	Cat#: 557403
MLN-8237	Selleck Chemicals	Cat#: S1133
NMS-873	Sigma-Aldrich	Cat#: SML-1128
Triptolide	Sigma-Aldridch	Cat#: T3652
Critical commercial assays		
TnT Sp6-coupled rabbit reticulocyte system	Promega	Cat#: L2080
Protein A Dynabeads	Fisher	Cat#: 10-002-D
NEBNext Ultra II DNA library Prep Kit for Illumina	New England Biolabs	Cat#: E76452
SuperScript III First Strand Synthesis system	Thermo Fisher Scientific	Cat#: 18080051
RNeasy Mini kit	Qiagen	Cat#: 74104
Deposited data		
Xenopus laevis ChIP-seq	Smith et al.[26] and Bredeson et al.[72]	NCBI GEO: GSE153058
Xenopus tropicalis ChIP-seq	Smith et al.[26] and Bredeson et al.[72]	NCBI GEO: GSE199671
Xenopus borealis ChIP-seq	This paper	NCBI BioProject: PRJNA848409

(*Continued on next page*)

Continued

REAGENT or RESOURCE	SOURCE	IDENTIFIER
Experimental models: Organisms/strains		
Xenopus laevis	Nasco	Cat#: LM00535
Xenopus laevis	National *Xenopus* Resource	Cat#: NXR_0031
Xenopus tropicalis	Nasco	Cat#: LM00822
Xenopus tropicalis	National *Xenopus* Resource	Cat#: NXR_1018
Xenopus borealis	Nasco	Cat#: LM00698
Oligonucleotides		
Primers (FCR monomer sequence amplification, pJET1.2 Sequencing Primers) FWD: CGA CTCACTATAGGGAGAGCGGC REV: AAG AACATCGATTTTCCATGGCAG	Smith et al.[26]	N/A
Primers (*X. laevis* CENP-A amplification) FWD: CAAGCTTCGAATTCTGCAGTCGA CTGCCACCATGAGACCGGGCTCCACTCC REV: GGGTTAATGAGGGACTGGGGTAAG AGCCTCTAGAACTATAGTGAGTCGTATTAC	This paper	N/A
Primers (*X. tropicalis* CENP-A amplification) FWD: CAAGCTTCGAATTCTGCAGTCGACT GCCACCATGAGGCCTGGGTCTACTCC REV: (GAGTTACTGAGGGGTTGGGGTAAG AGCCTCTAGAACTATAGTGAGTCGTATTAC)	This paper	N/A
Primers (*X. borealis* CENP-A amplification) FWD: TAAGCACTCGAGGCCATGAGATCGG GGTCCACTCCREV: AATCGTTCTAGAGGCT TACCCCAGTCCCTCATTAACCC	This paper	N/A
Recombinant DNA		
Plasmid: Full length *X. laevis* CENP-A in pCS2+ vector	This paper	N/A
Plasmid: Full length *X. tropicalis* CENP-A in pCS2+ vector	This paper	N/A
Plasmid: Full length *X. borealis* CENP-A in pCS2+ vector	This paper	N/A
Plasmid: Full length *X. laevis* GFP-xHJURP in pCS2+ vector	Straight Lab	ASP1640
Plasmid: Full length *X. laevis* xCENP-C-myc in pCS2+ vector	Straight Lab	ASP867
Plasmid: FCR monomer4 in pJET1.2	Straight Lab[26]	N/A
Plasmid: FCR monomer10 in pJET1.2	Straight Lab[26]	N/A
Plasmid: FCR monomer16 in pJET1.2	Straight Lab[26]	N/A
Plasmid: FCR monomer19 in pJET1.2	Straight Lab[26]	N/A
Software and algorithms		
FIJI	Schindelin et al.[73]	https://imagej.net/software/fiji/
Matlab		https://www.mathworks.com/products/matlab.html
k-mer counting pipeline	Smith et al.[26]	https://github.com/straightlab/xenla-cen-dna-paper
cd-his-est	Fu et al.[74]	http://weizhong-lab.ucsd.edu/cd-hit/
Geneious (7.1.4)		https://www.geneious.com/
RepeatMasker 4.0.9	Smit et al.[75]	http://www.repeatmasker.org

RESOURCE AVAILABILITY

Lead contact

Further information and requests for resources and reagents should be directed to and will be fulfilled by the lead contact, Rebecca Heald (bheald@berkeley.edu).

Materials availability

All materials are available upon request. In general, plasmid constructs and antibodies are available for sharing.

Data and code availability

ChIP-seq data used in this study are publicly available at NCBI. Accession numbers are listed in the key resources table.

EXPERIMENTAL MODEL AND SUBJECT DETAILS

All frogs were used and maintained in accordance with standards established by the UC Berkeley Animal Care and Use Committee and approved in our Animal Use Protocol. Mature *Xenopus laevis*, *X. tropicalis*, and *X. borealis* frogs were obtained from Nasco (Fort Atkinson, WI) or the National *Xenopus* Resource (Woods Hole, MA). *Xenopus* frogs were housed in a recirculating tank system with regularly monitored temperature and water quality (pH, conductivity, and nitrate/nitrite levels). *X. laevis* and *X. borealis* were housed at 20-23°C, and *X. tropicalis* were housed at 23-26°C. All animals were fed Nasco frog brittle.

Chemicals

Unless otherwise states, all chemicals were purchased from Sigma-Aldrich, St. Louis, MO.

Frog care

X. laevis, *X. tropicalis*, and *X. borealis* females were ovulated with no harm to the animals with a 6-, 3-, and 4-month rest interval, respectively, as previously described.[76] To obtain testes, males were euthanized by over-anesthesia through immersion in ddH_2O containing 0.15% MS222 (Tricaine; Sigma) neutralized with 5 mM sodium bicarbonate prior to dissection, and then frozen at -20°C.

METHOD DETAILS

CENP-A ChIP-seq and data analysis

CENP-A MNase ChIP-seq was performed as previously described.[26] Briefly, livers were extracted from adult *X. borealis* animals and flash frozen. Upon thawing, livers were diced on ice, rinsed in PBS, and buffer 1 (2.5 mM EDTA, 0.5 M EGTA, 15 mM Tris-HCl pH 7.4, 15 mM NaCl, 60 mM KCl, 15 mM sodium citrate 0.5 mM spermidine, 0.15 mM spermine, 340 mM sucrose, supplemented with 0.1 mM PMSF) was added and the tissue dounced using pestle A 12 times. A syringe with 18-gauge needle was backfilled with nuclei mixture and expelled into 2 mL tubes with additional buffer 1. Nuclei were spun at 6,000g for 5 min at 4°C, and washed 3 times with buffer 3 (2.5 mM EDTA, 0.5 M EGTA, 15 mM Tris-HCl pH 7.4, 15 mM NaCl, 60mM KCl, 15 mM sodium citrate 0.5 mM spermidine, 0.15 mM spermine, 340 mM sucrose, supplemented with 0.1 mM PMSF). Nuclei quality was checked and nuclei were counted by hemocytometer. ~5-10 million nuclei were used per IP reaction.

For MNase digestion, $CaCl_2$ was added to each reaction tube to 5 mM together with 300 U of MNase. Digestion was performed at RT for 30 min and reaction was quenched with 10 mM EDTA and 5 mM EGTA. Nuclei were lysed with 0.05% IGEPAL CA-630 in ice for 10 min. Following an initial spin 1,500g 5 min 4°C, the pellet was resuspended in 500 μL buffer 3 + 200 mM NaCl and rotated overnight at 4°C to extract mononucleosomes. Samples were precleared, input fractions were taken and CENP-A mononucleosomes were isolated with 10 μg rabbit anti *X. laevis* CENP-A antibody prebound to protein A dynabeads in 200 μL TBST with rotation overnight at 4°C. Beads were washed and eluted, mononucleosomal DNA was isolated with Ampure beads, and sequencing libraries were prepared using NEBNext fit for Illumina sequencing which was performed on a NovaSeq instrument with paired end 150bp sequencing.

X. laevis and *X. tropicalis* CENP-A CHIP-seq datasets were used from previously described studies.[26,72] CENP-A ChIP and Input libraries from each species were processed to identify CENP-A enriched *k*-mers using the k-mer counting pipeline that normalizes k-mer counts by sequencing depth of each library (https://github.com/straightlab/xenla-cen-dna-paper). For this study 25bp *k*-mers were used and kmc was run with ci=10, indicating that *k*-mers must be found 10 times in the dataset to be considered. This was chosen so that more *k*-mers were identified from each species to make comparisons more likely.

A phylogram was generated using a method similar to that previously described.[26] From each species full length ChIP-seq reads were selected based on the presence of at least 80 CENP-A enriched *k*-mers. The reads from each species that met this criterion were then clustered by sequence similarity using cd-hit-est[74] using sequential rounds of clustering by 98%, 95%, and 90% identical by sequence. The 20 top clusters from each species were then selected for phylogram generation using Geneious (7.1.4) Tree Builder with the following settings: Genetic Distance Model=Tamura-Nei, Tree building method=Neighbor-joining, Outgroup=No outgroup, Alignment Type=Global alignment, Cost Matrix=93% similarity. Colors for each species were added manually.

To identify repeat classes enriched in the CENP-A datasets from each species, RepeatMasker 4.0.9[75] was run using the giri Repbase library for *Xenopus* repeats on subsets of one million reads generated from CENP-A and Input sequencing libraries in triplicate. Counts for each repeat class were summarized and an enrichment score of CENP-A/Input was calculated for each pair of subsets. Enrichment scores for each repeat class were reported as a bar plot of the mean and standard deviation of the triplicates for each species.

Protein sequence alignments

Multiple sequence alignments were performed using Clustal Omega (default parameters). Sequence similarities were determined by pair-wise alignments using EMBOSS Needle (default parameters).

Xenopus egg extracts

X. laevis and *X. tropicalis* metaphase-arrested egg extracts and spindle reactions were prepared as previously described.[37,77,78] Briefly, freshly laid, metaphase II-arrested eggs were collected, dejellied, packed and crushed by centrifugation. The cytoplasmic layer was collected with a syringe and 18G needle, then supplemented with 10 μg/mL of leupeptin, pepstatin, and chymostatin (LPC), 20 μM of cytochalasin B, and energy mix (3.75 μM creatine phosphate, 0.5 μM ATP, 0.5 μM $MgCl_2$, 0.05 μM EGTA). Typical reactions contained 20 μL CSF extract, sperm nuclei at a final concentration of 500 nuclei/μL, and rhodamine-labeled porcine brain tubulin at a final concentration of 50 μg/mL.

Chromosome immunofluorescence

Spindle reactions were prepared, spun-down, and processed for immunofluorescence as previously described.[37,77] Briefly, the extract reactions were fixed for 5–10 min with 2% formaldehyde and spun down at 5,500 rpm (5821.9 x g) for 20 min at 16°C. The coverslips were incubated for 30 s in cold methanol, washed in PBS + 0.1% NP40, and blocked overnight in PBS + 3% BSA at 4°C. We used rabbit anti-xCENPA, 1:500,[15,40] mouse anti-myc (9E10 clone, 1:500), rabbit anti-POLR1A (Novus Biologicals, 1:500), and mouse anti-UBTF (Abnova, 1:500) antibodies. Primary antibodies were added for 1 h in PBS + 3% BSA. After washing with PBS + 0.1% NP40, the coverslips were incubated with 1:1000 anti-rabbit or mouse secondary antibodies coupled to Alexa Fluor 488 or 568 (Invitrogen), respectively, for 30 min and then with 1:1000 Hoechst (Invitrogen) for 5 min. The coverslips were then washed and mounted for imaging with Vectashield (Vector Labs). Each presented dataset was obtained from three independent egg extracts.

Nuclear DNA FISH for FCR centromeric sequences

Nuclear DNA FISH using probes against various FCR monomers was performed as previously described.[26] Briefly, pJET1.2 plasmids containing 150 bp FCR monomer sequences were PCR-amplified and fluorescently labeled using random hexamer priming and Klenow (exo-) polymerase (New England Biolabs). Both Alexa Fluor 488 and 568 dUTP-conjugated fluorophores (Invitrogen) were used. Probes were desalted to remove unincorporated nucleotides, then precipitated and cleaned before resuspension in hybridization buffer (65% formamide, 5X SSC, 5X Denhardts with 1% blocking reagent (Roche), 0.5 mg/mL salmon sperm DNA added fresh). Each experiment used 4 uL of probe mixed with 4 uL of hybridization buffer.

Nuclei were assembled in egg extract, spun down onto coverslips, and probed with CENP-A antibody as previously described in Levy and Heald [79] and detailed above. Samples proceeded to FISH by fixation in 2.5% formaldehyde in PBS for 10 min, washed in PBS, and dehydrated with increasing concentrations of 70-100% ice-cold ethanol. Coverslips were blocked for 30 m in hybridization buffer. Probes were warmed and mixed with hybridization buffer before being added to samples, flipping coverslips onto glass slides for hybridization. These ''sandwiches'' were incubated at 80°C for 10 min, then incubated overnight at 37°C. Coverslips were removed from glass slides carefully with 4X SSC, washed thoroughly in SSC, stained with Hoechst and mounted with Vectashield (Vector Labs).

Protein expression in reticulocyte lysate

To generate plasmids for expression of species-specific *X. laevis*, *X. tropicalis*, and *X. borealis* CENP-A, total RNA was isolated from stage 9 embryos. Embryos were homogenized mechanically in TRIzol (Thermo Fisher Scientific) using up to a 30-gauge needle and processed according to manufacturer's instructions. After resuspension in nuclease-free H2O, RNAs were cleaned using a RNeasy kit (Qiagen) according to manufacturer's instructions, and cDNA was synthesized using the SuperScript III First Strand Synthesis system (Thermo Fisher Scientific) according to the manufacturer's instructions. The *X. laevis*, *X. tropicalis*, and *X. borealis* CENP-A sequences were then PCR-amplified from the cDNA. The amplified sequence was then subcloned into a pCS2+ vector using Gibson assembly. The constructs were then amplified using XL1-Blue competent *E. coli* (Agilent).

The TnT Sp6-coupled rabbit reticulocyte system (Promega) was used for in vitro transcription/translation (IVT) of plasmid DNA according to the manufacturer's protocol. 2–10% of the final egg extract reaction volume was added prior to addition of sperm nuclei; for CENP-A, this corresponds to 8-80 times endogenous protein levels.

Western blots

Increasing volumes of egg extracts and reticulocyte lysate were subject to SDS-PAGE and wet transferred to PVDF membranes. Blots were blocked with PBS + 0.1% Tween + 5% milk for 1 h, probed with primary antibodies diluted in PBS + 0.1% Tween + 5% milk for 1 h, rinsed 3x over a 10 m period with PBS + 0.1% Tween, then probed with secondary antibodies (Rockland Immunochemicals; goat anti-rabbit DyLight 800 and donkey anti-mouse DyLight 680, 1:10,000) diluted in PBS + 0.1% Tween for 30 m. Blots were scanned on an Odyssey Infrared Imaging System (Li-Cor Biosciences). Band intensities were quantified using FIJI.

Drug treatments

X. tropicalis extract was supplemented with the following drugs and concentrations: Aphidicolin (DNA replication inhibitor, 10 μg/mL, Sigma), BMH-21 (RNA Polymerase I inhibitor, 1 μM, Sigma), NMS-873 (p97 inhibitor, 10 μM, Sigma), MLN-8237 (Aurora A inhibitor, 1 μM, Selleck Chemicals), BI-2536 (Polo kinase 1 inhibitor, 1 μM, Selleck Chemicals), Triptolide (RNA Polymerase II inhibitor, 25 μM, Sigma).

Chromosome and nuclei imaging

Chromosomes were imaged using Micromanager 1.4 software[80] and nuclei were imaged using Olympus cellSens Dimension 2 software on an upright Olympus BX51 microscope equipped with an ORCA-ER or ORCA-Spark camera (Hamamatsu Photonics) and Olympus UPlan 60x/NA 1.42 oil objective. All images across all datasets were taken using the same exposure settings.

In vitro fertilization and cross-fertilizations

In vitro fertilization and cross-fertilizations were performed as previously described.[25,76,81] *X. laevis*, *X. borealis*, and *X. tropicalis* males were injected with 500, 300, and 250 U, respectively, of human chorionic gonadotropin hormone (hCG, Sigma) 12-24 h before dissection. Testes were collected in Leibovitz L-15 Medium (Gibco, Thermo Fisher Scientific) supplemented with 10% fetal bovine serum (FBS; Gibco) for immediate use. *X. tropicalis* females were primed with 10 U of hCG 12-18 h before use and boosted with 250 U of hCG on the day of the experiment. As soon as the first eggs were laid (~3 h after boosting), the male was euthanized and dissected. Two *X. tropicalis* testes or one *X. laevis* or *X. borealis* testis were added to 1 mL of L-15 + 10% FBS. *X. tropicalis* females were squeezed gently to deposit eggs onto glass Petri dishes (Corning) coated with 1.5% agarose in 1/10X MMR (1X MMR: 100 mM NaCl, 2 mM KCl, 2 mM CaCl2, 1 mM MgSO4, 0.1 mM EDTA, 5 mM HEPES-NaOH pH 7.6). Testes were homogenized using a pestle in L-15 + 10% FBS to create sperm solution. Any liquid in the Petri dishes was removed, and the eggs were fertilized with 500 uL of sperm solution per dish. Eggs were swirled in the solution to separate them and incubated for 5 min with the dish slanted. Dishes were flooded with ddH_2O and incubated for 10 min. ddH_2O was exchanged for 1/10X MMR and incubated for 10 min. The jelly coats were removed with a 3% cysteine solution (in ddH_2O-NaOH, pH 7.8). After extensive washing with 1/10X MMR (at least four times), embryos were incubated at 23°C until the first cleavage at 1 hour post fertilization (hpf). Fertilized embryos were then sorted and placed in a mesh-bottomed dish for microinjection as described below.

Embryo microinjection

At stage 2 (2-cell embryo), embryos were transferred to a 1/9X MMR + 3% Ficoll. IVT reticulocyte lysate was backloaded into a needle pulled from a 1 mm glass capillary tube (TW 100F-4, World Precision Instruments) using a P-87 Micropipette Puller (Sutter Instrument). Embryos were placed in a mesh-bottomed dish and microinjected in both blastomeres with 2 nL of the IVT reticulocyte lysate using a Picospritzer III microinjection system (Parker) equipped with a MM-3 micromanipulator (Narishige). Injected embryos were transferred to a new dish and incubated at 23°C in 1/9X + 3% Ficoll for several hours, then buffer exchanged for 1/10X MMR overnight.

Embryo video imaging

Imaging dishes were prepared using an in-house PDMS mold designed to print a pattern of 0.9 mm large wells in agarose that allowed us to image six *X. tropicalis* embryos simultaneously within the 3 mm x 4 mm camera field of view for each condition. Embryos were imaged from stage 3 after microinjection. Treatment and control videos were taken simultaneously using two AmScope MD200 USB cameras (AmScope), each mounted on an AmScope stereoscope. Time-lapse movies were acquired at a frequency of one frame every 10 s for 20 h and saved as Motion JPEG using a Matlab (The MathWorks) script. Movie post-processing (cropping, concatenation, resizing, and addition of scale bar) was done using Matlab and FIJI.[73] All Matlab scripts written for this study are available upon request. Two of the scripts used here were obtained through the MATLAB Central File Exchange: 'videoMultiCrop' and 'concatVideo2D' by 'Nikolay S'.

Embryo whole-mount immunofluorescence

Embryos were fixed at the desired stages for 1-3 h using MAD fixative (2 parts methanol, Thermo Fisher; 2 parts acetone, Thermo Fisher; 1 part DMSO, Sigma). After fixation, embryos were dehydrated in methanol and stored at -20°C. Embryos were then processed for immunofluorescence as previously described.[25] Briefly, embryos were gradually rehydrated in 0.5X SSC (1X SSC: 150 mM NaCl, 15 mM Na citrate, pH 7.0), then bleached with 2% H_2O_2 in 0.5X SSC with 5% formamide for 2 h under light. Embryos were washed with PBT (1X PBS, 0.1% Triton X-100, 2 mg/mL bovine serum albumin). Embryos were blocked in PBT supplemented with 10% goat serum and 5% DMSO for 1-3 h and incubated overnight at 4°C in PBT supplemented with 10% goat serum and primary antibodies. We used mouse anti-beta-tubulin (E7, Developmental Studies Hybridoma Bank, 1:300 dilution) and rabbit anti-histone H3 (Abcam, 1:500 dilution). Embryos were then washed 4 x 2 h in PBT and incubated overnight at 4°C in PBT supplemented with goat anti-mouse and goat anti-rabbit secondary antibodies coupled to Alexa Fluor 488 and 568 (Invitrogen). Embryos were then washed 4 x 2 h in PBT and gradually dehydrated in methanol. Finally, embryos were cleared in Murray's clearing medium (2 parts benzyl benzoate, Sigma; 1 part benzyl alcohol, Sigma). Embryos were placed in a reusable chamber (Thermo Fisher) for confocal microscopy.

Confocal microscopy

Confocal microscopy was performed on an inverted Zeiss LSM 800 using the Zeiss Zen software, a Plan-Achromat 20X/0.8 air objective and laser power 0.5-2%, on multiple 1024x1024 pixel plans spaced of 0.68 μm in Z. Images are mean averages of two scans with a depth of 16 bits. Pinhole size always corresponded to 1 Airy unit.

QUANTIFICATION AND STATISTICAL ANALYSIS

Quantification of CENP-A localization on mitotic chromosomes was determined manually in a dataset of 100 images from one extract. Quantification of ultra-thin chromosomal regions was also determined manually in parallel from the same datasets. Only

single chromosomes were counted. Each dataset had ~150-400 chromosomes. The average of each extract was calculated as a percentage of total chromosome number. Averages were plotted in Matlab, and statistical significance and p-values were determined with two-tailed, two-sample unequal variance t-tests or one-way ANOVA with Tukey post-hoc analysis in Microsoft Excel. The number of egg extracts used, individual chromosomes counted, and p-values are listed in the figure legends. For all box plots, the thick line inside the box indicates the average across biological replicates, and the upper and lower box boundaries indicate the standard deviation.

PolR1A and UBF fluorescent intensity on *X. borealis* ultra-thin chromosomes were quantified in FIJI by measuring the intensity of the stretched region specifically and comparing it to a random non-stretched region on the same chromosome. All intensity measurements were normalized to the samples' Hoechst intensity.

Micronuclei in embryos were quantified at the relevant stages as the number of observed micronuclei divided by the number of nuclei, counted manually in FIJI. Statistical significance was determined by two-tailed, two-sample unequal variance t-tests.